

## CHAPTER IV

### RESULTS AND DISCUSSIONS

#### 4.1 Catalyst Characterization

In this work, TTIP, TBT, and TEOT with their molecular weights of 284.2, 340.3, 228.1, respectively, were used as the TiO<sub>2</sub> precursors. They are different in the molecular weight and the rate of hydrolysis because of the difference in their molecular structure. TBT has the slowest hydrolysis rate because of its straight chain. TEOT has the highest hydrolysis rate because of its smaller molecular size.

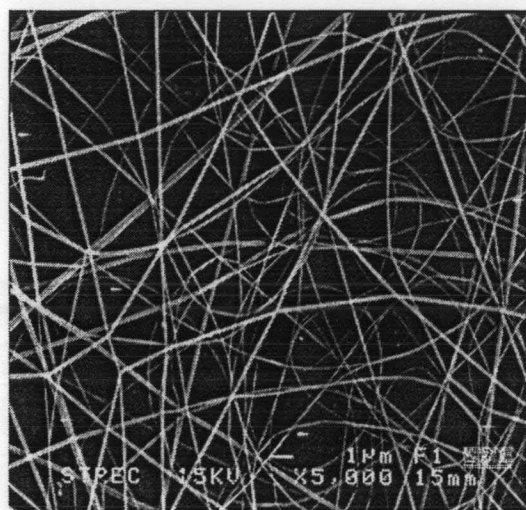
##### 4.1.1 Morphology of TiO<sub>2</sub> Nanofibers

Table 4.1 shows the average diameters of the TiO<sub>2</sub> nanofibers. The sizes of the as-spun TiO<sub>2</sub>/PVP composite nanofibers are not much different with the different Ti-precursors. Moreover, the sizes of the as-spun TiO<sub>2</sub>/PVP composite nanofibers are greater than that of the calcined-TiO<sub>2</sub> for all Ti-precursors because the content of PVP was removed from the fibers after the calcination. And when the calcination temperature increases, the calcined-TiO<sub>2</sub> nanofibers sizes remain relatively constant because PVP was completely removed from the fibers at 500°C.

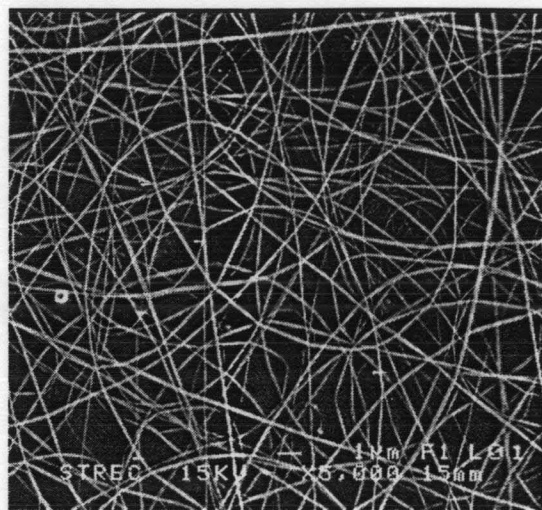
The SEM micrographs of the as-spun TiO<sub>2</sub>/PVP composites show that the fibers are smooth and long (Figure 4.1). But after the calcination, the fibers were cracked and shrunk (Figures 4.2-4.3).

**Table 4.1** Average diameters of TiO<sub>2</sub> nanofibers

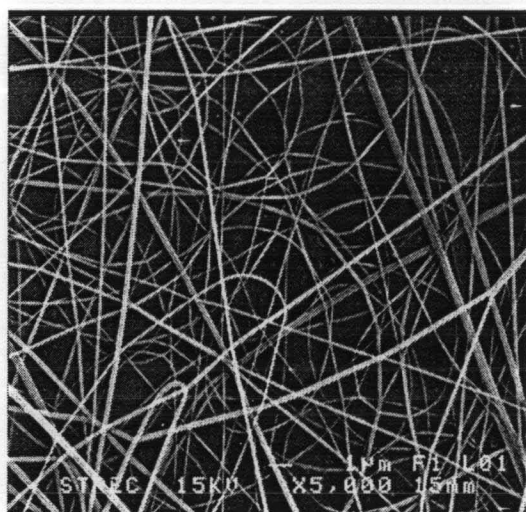
Type of Ti-precursors	Average diameter (nm)			
	As-spun TiO <sub>2</sub>	Calcined TiO <sub>2</sub>		
		500°C	600°C	700°C
TTIP	92.50±39.72	79.12±30.44	79.80±28.40	-
TBT	71.34±29.09	60.66±16.16	62.56±13.58	-
TEOT	89.62±28.64	64.86±25.15	67.52±23.42	-



(a)



(b)



(c)

**Figure 4.1** Scanning electron micrographs (SEM) of the as-spun  $\text{TiO}_2$  nanofibers: (a) TTIP (b) TBT (c) TEOT.

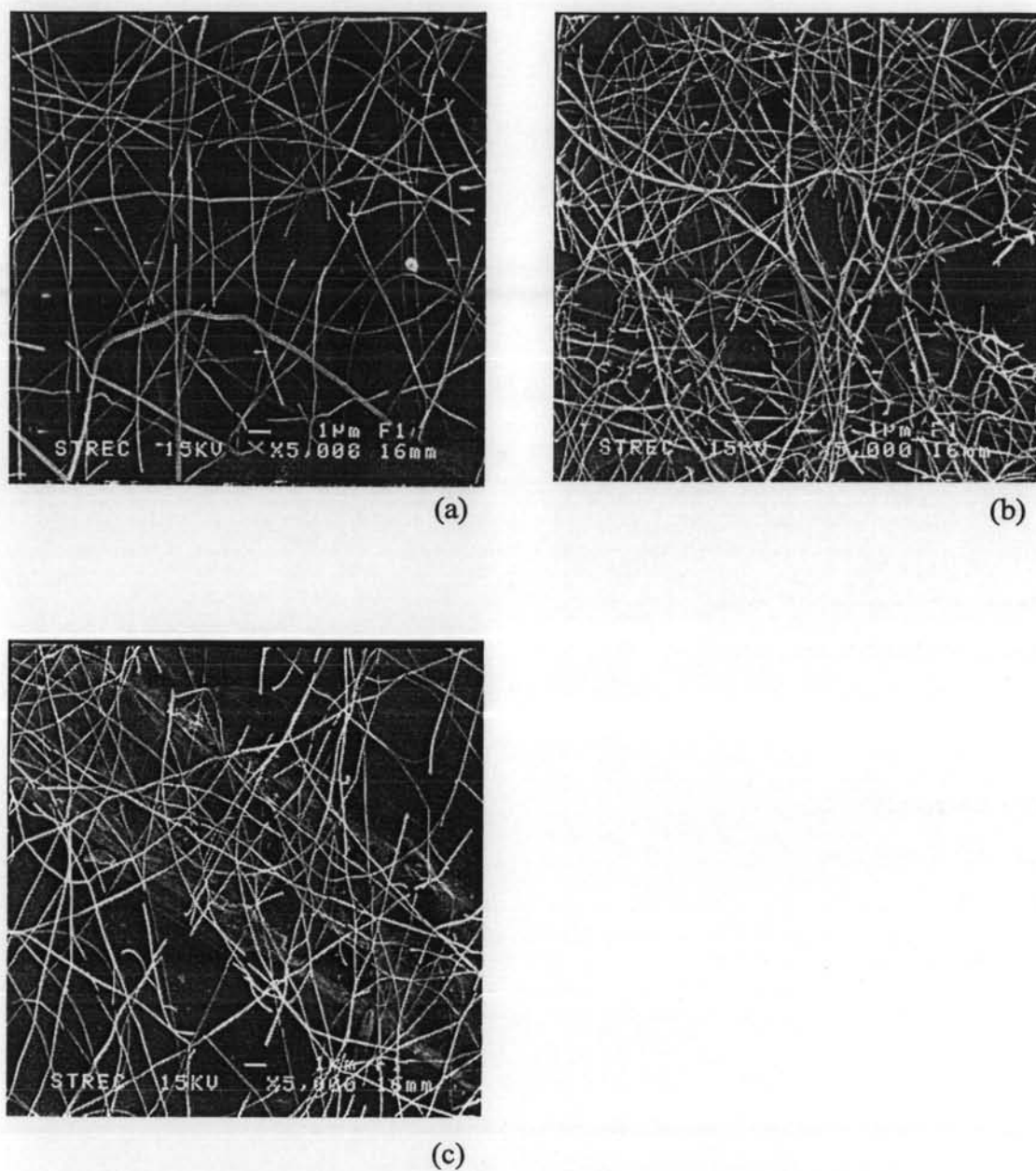


**Figure 4.2** Scanning electron micrographs (SEM) of the  $\text{TiO}_2$  nanofibers after the calcination at  $500^\circ\text{C}$ : (a) TTIP (b) TBT (c) TEOT.

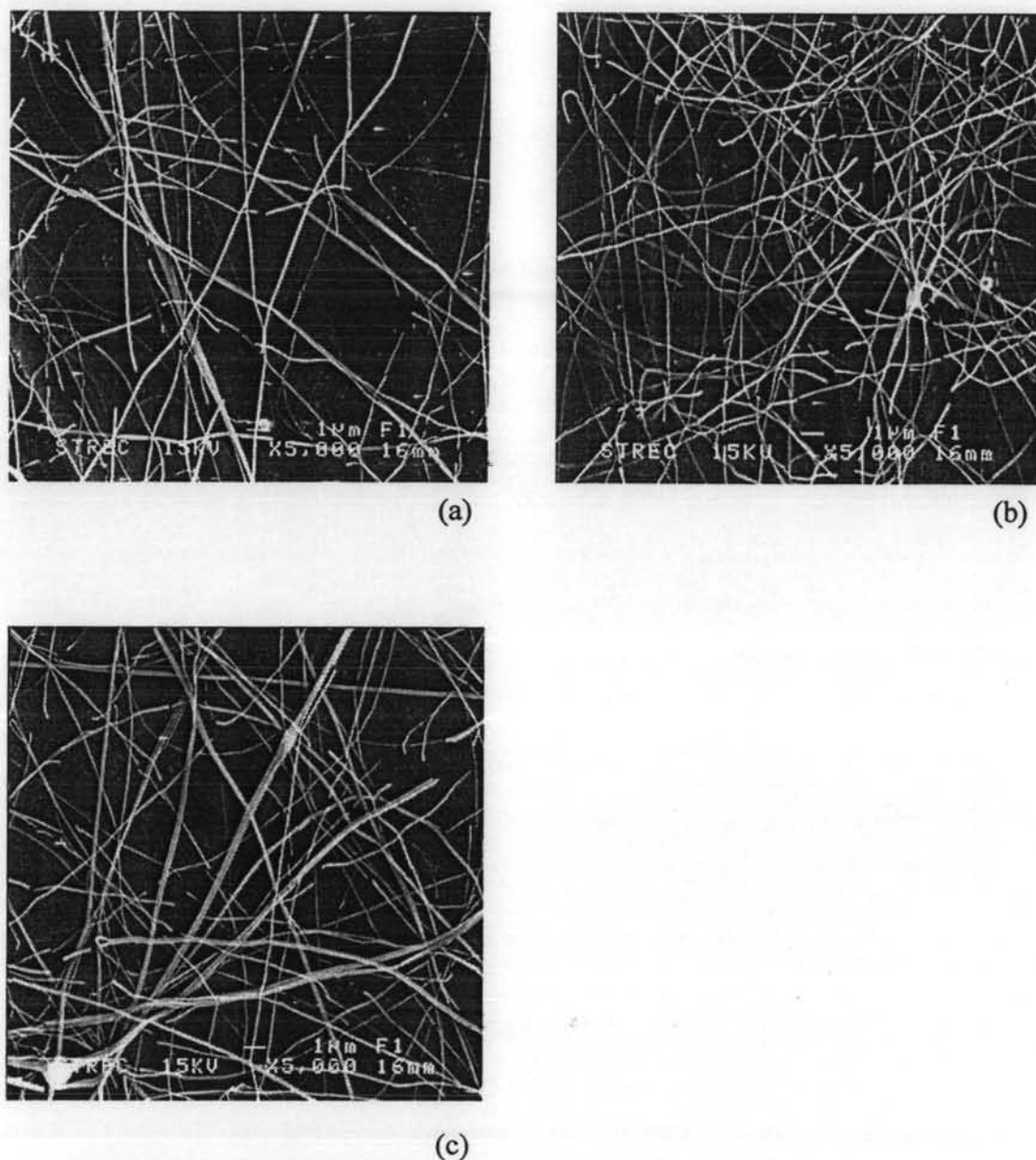


**Figure 4.3** Scanning electron micrographs (SEM) of the  $\text{TiO}_2$  nanofibers after the calcination at  $600^\circ\text{C}$ : (a) TTIP (b) TBT (c) TEOT.

#### 4.1.2 Crystal Structure

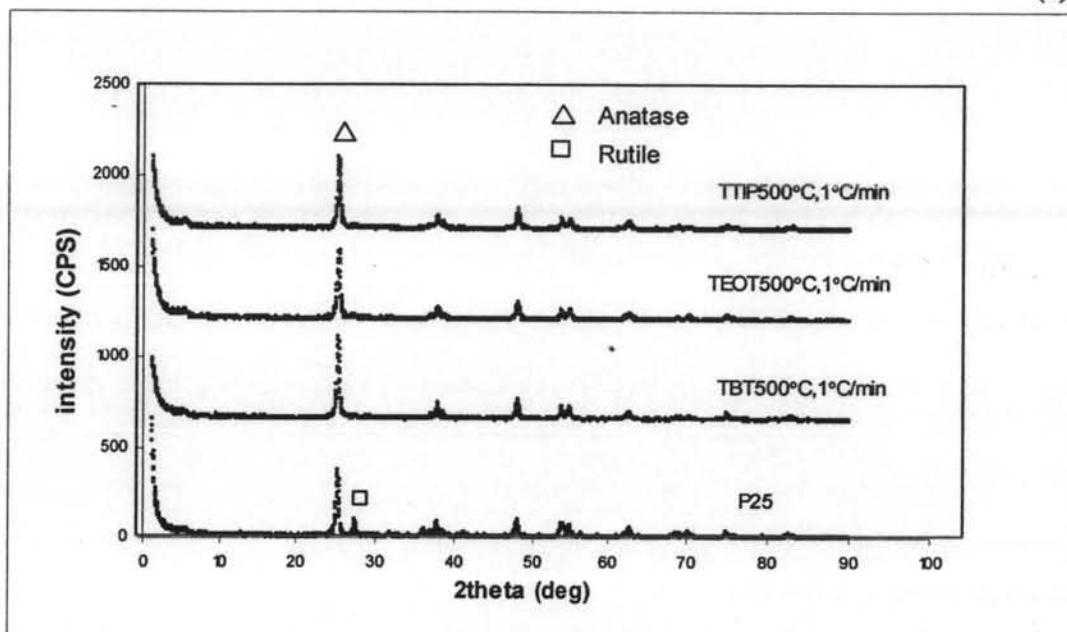
Figure 4.4 shows the XRD patterns of the  $\text{TiO}_2$  nanofibers prepared with different Ti-alkoxides at different calcination temperatures ( $500$ ,  $600$ , and  $700^\circ\text{C}$ ) and compared with the commercial  $\text{TiO}_2$  (Degussa P25). For the XRD patterns of  $\text{TiO}_2$ , the main peaks of anatase, rutile, brookite are at  $2\theta = 25.3^\circ$ ,  $27.5^\circ$ ,

and 30.6°, respectively. The TiO<sub>2</sub> (Degussa P25) shows two phases of anatase and rutile.

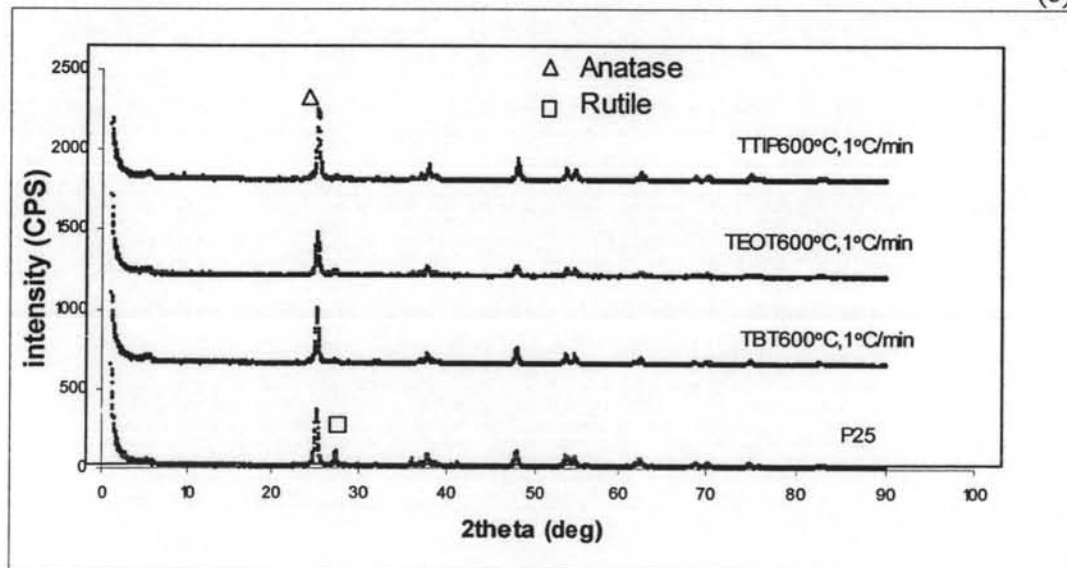
It was found that at the calcination temperature of 500°C, TiO<sub>2</sub> prepared from all the Ti-alkoxides has only the anatase phase. At 600°C, only TEOT forms a small percentage of rutile and at 700°C, all TiO<sub>2</sub> has more rutile content. Table 4.2 indicates that the composition of anatase is the least in the case of using TTIP and calcination at 700°C. This suggests that the phase changes from anatase to rutile rapidly. Moreover, adding a small amount of Ag, the more rutile content is observed. And the sizes of anatase phase are insignificantly smaller than TiO<sub>2</sub> without adding Ag.

The crystallite sizes of the catalysts can be determined from the broadening of main peak by the Debye-Scherrer equation. The crystallite sizes of the catalysts are shown in Table 4.2. It indicates that for the same Ti-alkoxides the crystallite size of anatase increases with the increase in the calcination temperature. The comparison among the three types of Ti-precursors at the 500°C and 600°C calcination temperature shows that using TTIP as the Ti-precursors resulted in the largest sizes of anatase. It can be explained that the structure of TTIP has more branches than the others. So, during the formation of TiO<sub>2</sub>, the grain growth may be larger than that from TEOT (the smaller structure) and TBT (straight chain). But for the calcination at 700°C, the same size of anatase phase can be observed because during such the high calcination temperature, each of the small grain boundary agglomerates together until it cannot do so anymore at 700°C. However, Degussa P25 still has the smallest size of the anatase form.

(a)



(b)



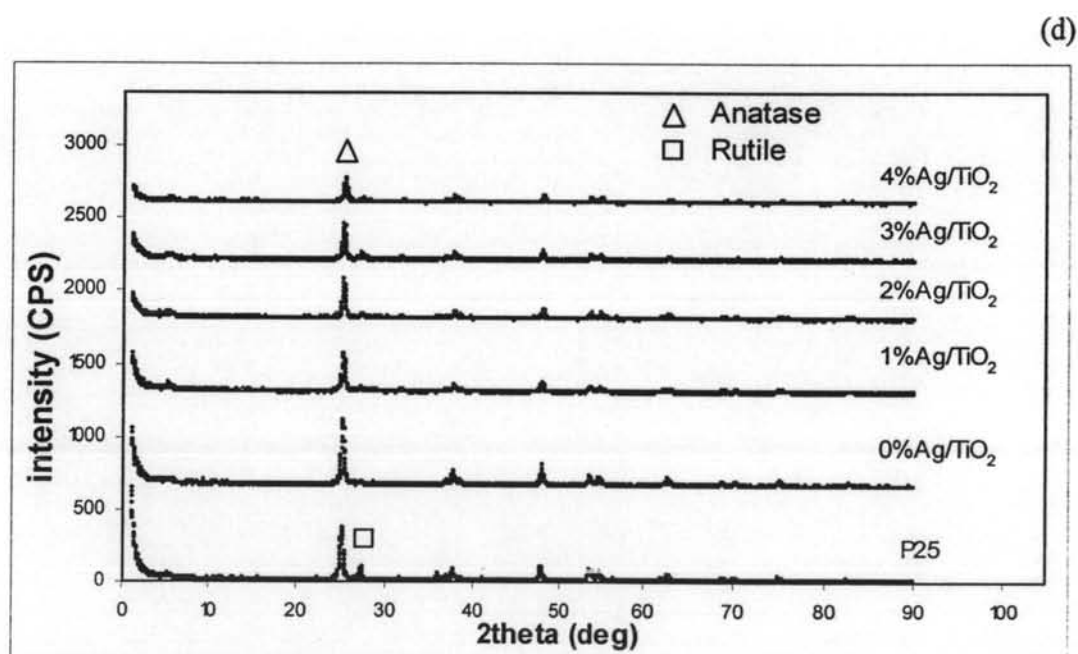
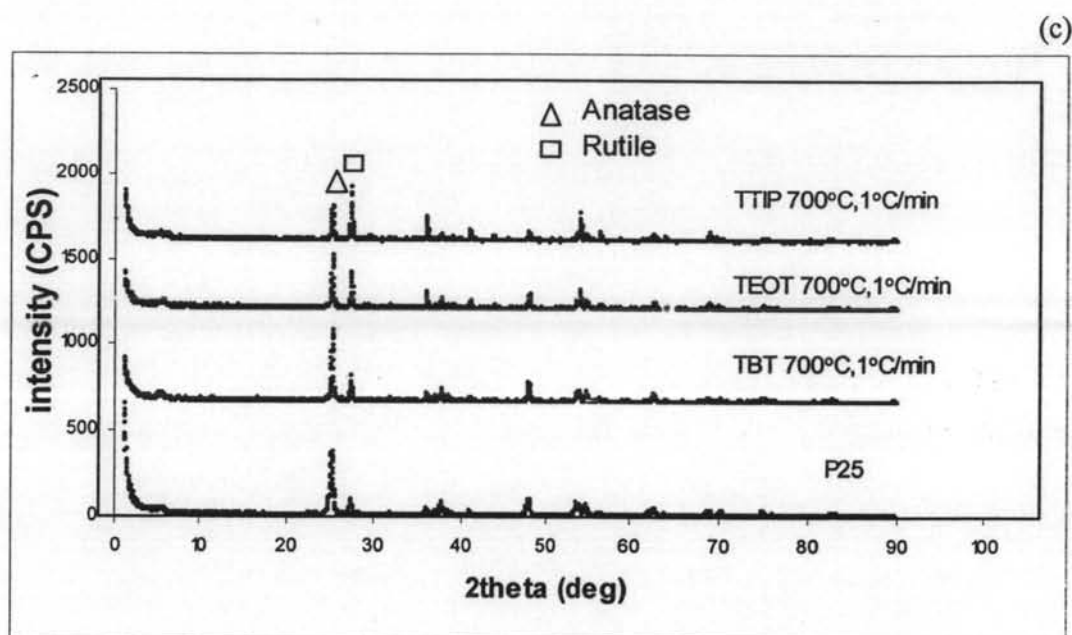


**Figure 4.4** X-ray diffraction patterns of the TiO<sub>2</sub> nanofibers prepared with different Ti-alkoxide after the calcination and Degussa P25; (a) 500°C (b) 600°C (c) 700°C (d) Ag doped TiO<sub>2</sub>.

**Table 4.2** Crystallite sizes of the TiO<sub>2</sub> nanofibers and Degussa P25

Catalyst	Crystallite size (nm)		%Anatase*
	Anatase	Rutile	
TiO <sub>2</sub> (DegussaP25)	25.6	32.2	80.03
TiO <sub>2</sub> (TTIP 500°C,1°C/min)	32.5	-	-
TiO <sub>2</sub> (TBT 500°C,1°C/min)	27.5	-	-
TiO <sub>2</sub> (TEOT 500°C,1°C/min)	27.5	-	-
TiO <sub>2</sub> (TTIP 600°C,1°C/min)**	32.1	-	-
TiO <sub>2</sub> (TBT 600°C,1°C/min)	28.9	-	-
TiO <sub>2</sub> (TEOT 600°C,1°C/min)	34.2	64.4	78.16
TiO <sub>2</sub> (TTIP 700°C,1°C/min)	37.7	55.0	37.14
TiO <sub>2</sub> (TBT 700°C,1°C/min)	37.7	55.0	73.11
TiO <sub>2</sub> (TEOT 700°C,1°C/min)	37.7	55.0	57.48
1%Ag/TiO <sub>2</sub>	31.5	76.9	90.83
2%Ag/TiO <sub>2</sub>	31.5	52.8	89.10
3%Ag/TiO <sub>2</sub>	31.5	64.4	84.87
4%Ag/TiO <sub>2</sub>	29.3	64.4	86.94

\*(Jung and Park, 1999), \*\* the same condition as in the Ag doped TiO<sub>2</sub>

#### 4.1.3 Specific Surface Area (BET)

Table 4.3 shows specific surface areas (BET) of the TiO<sub>2</sub> nanofibers and Degussa P25. It was found that, at the calcination temperature 500°C, TiO<sub>2</sub> from TEOT has the highest BET surface areas; however, it is lower than the surface area of Degussa P25, because TiO<sub>2</sub> from TEOT has the highest rate of hydrolysis. During the electrospinning process, TEOT is injected through the nozzle into oxide's nanofibers of Ti immediately. Therefore, after the electrospinning process, most if not all electrospun fibers change into oxide of Ti. In the case of using TBT as a precursor, it was found that, at the calcination temperature 500°C, it has the BET surface areas close to that of the calcination temperature 600°C, because it has the lowest hydrolysis rate. Therefore, during the electrospinning process, there are some



electrospun fibers in the inner layer of fiber-mats that is not exposed to the moisture and still in the form of alkoxide.

With the same Ti-precursor, an increase in the calcination temperature, the BET surface area decreases because the grain agglomerates and results in the decrease in the BET surface area. Furthermore, doping of 1% and 2%Ag in TiO<sub>2</sub> increases the surface area. But adding Ag more than 2 wt% decreases the surface area as some Ag might block the pore structure of TiO<sub>2</sub>.

**Table 4.3** Specific surface areas of the TiO<sub>2</sub> nanofibers and Degussa P25

Catalyst	BET (m <sup>2</sup> /g)	Pore volume(cm <sup>3</sup> /g)	Pore size (A <sup>o</sup> )
TiO <sub>2</sub> (DegussaP25)	62.43	0.23	170.3
TiO <sub>2</sub> (TTIP 500°C,1°C/min)	48.58	0.16	131.6
TiO <sub>2</sub> (TTIP 600°C,1°C/min)	34.67	0.14	156.6
TiO <sub>2</sub> (TTIP 700°C,1°C/min)	17.91	0.06	123.9
TiO <sub>2</sub> (TBT 500°C,1°C/min)	43.46	0.18	163.9
TiO <sub>2</sub> (TBT 600°C,1°C/min)	43.02	0.16	154.0
TiO <sub>2</sub> (TBT 700°C,1°C/min)	24.84	0.10	162.1
TiO <sub>2</sub> (TEOT 500°C,1°C/min)	54.20	0.18	130.0
TiO <sub>2</sub> (TEOT 600°C,1°C/min)	44.71	0.15	137.5
TiO <sub>2</sub> (TEOT 700°C,1°C/min)	25.25	0.08	122.0
1%Ag/TiO <sub>2</sub>	39.80	0.15	147.5
2%Ag/TiO <sub>2</sub>	34.91	0.12	137.6
3%Ag/TiO <sub>2</sub>	30.32	0.13	129.9
4%Ag/TiO <sub>2</sub>	27.86	0.08	123.1

## 4.2 Photocatalytic Degradation of 4-CP

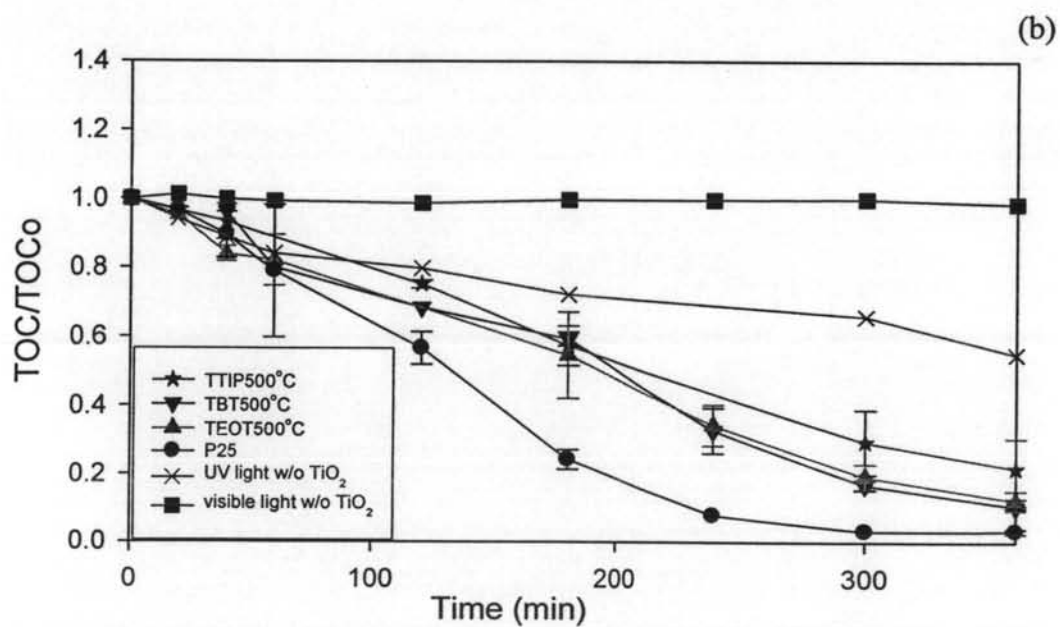
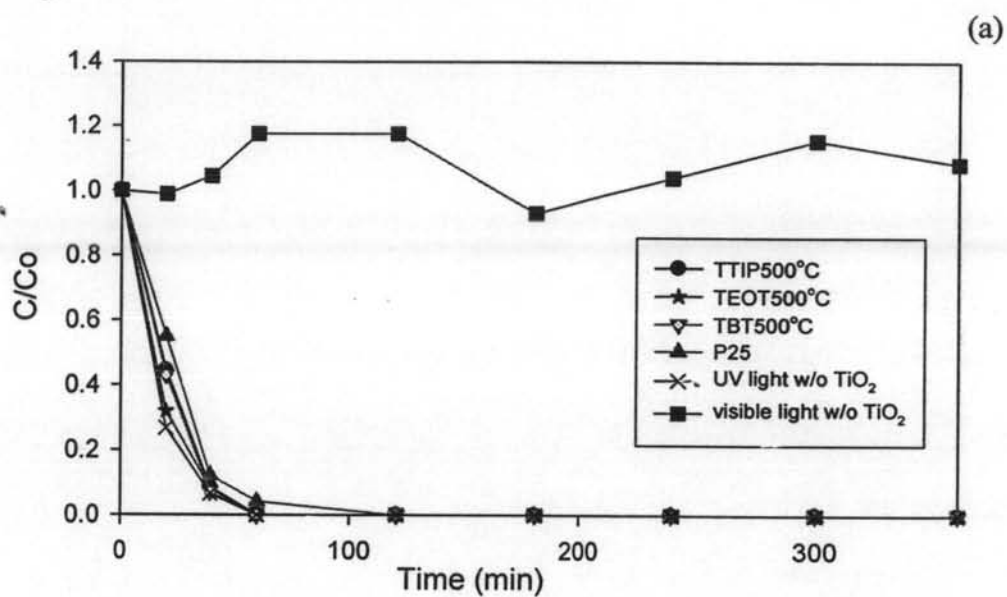
Some nomenclatures used throughout this section are the remaining fraction of 4-CP ( $C/C_0$ ) and the remaining fraction of TOC ( $TOC/TOC_0$ ).  $C/C_0$  is the ratio of 4-CP concentration at any times to its initial concentration. Similarly,  $TOC/TOC_0$  is the ratio of TOC concentration at any time to its initial concentration.

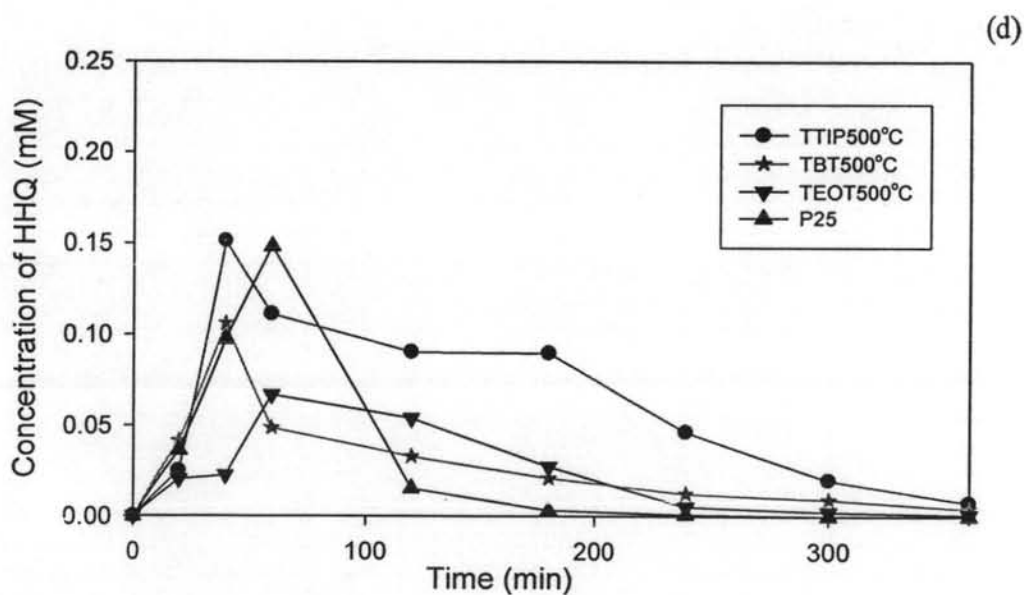
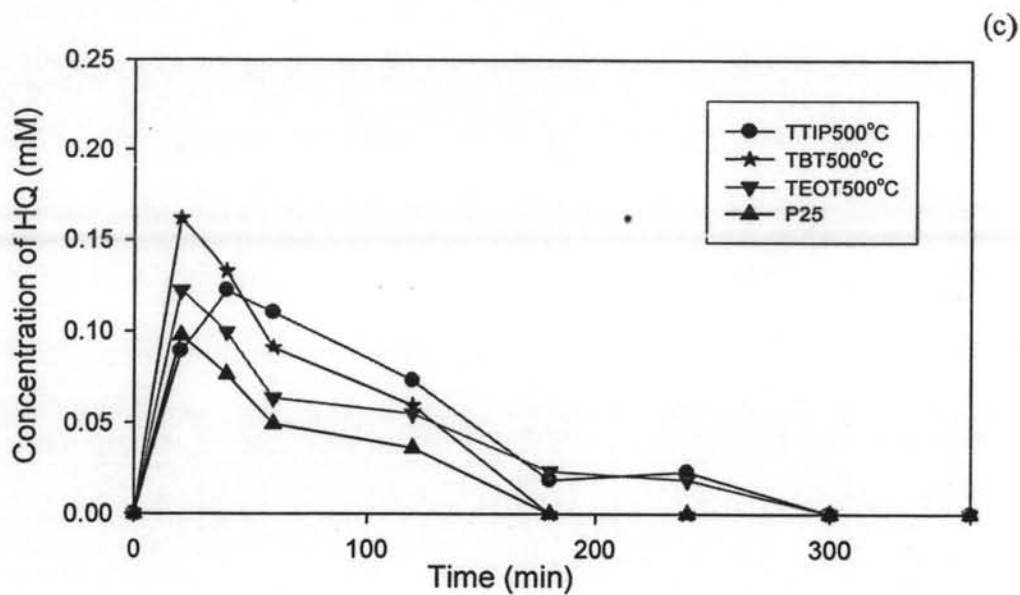
The photocatalytic degradations of 0.5 mM of 4-CP in aqueous solution by suspended 0.4 g/l of catalysts ( $\text{TiO}_2$  and Ag doped  $\text{TiO}_2$ ) under UV radiation (200-280 nm) were investigated and shown in Figures 4.5-4.16.

#### 4.2.1 Effect of Ti-precursors

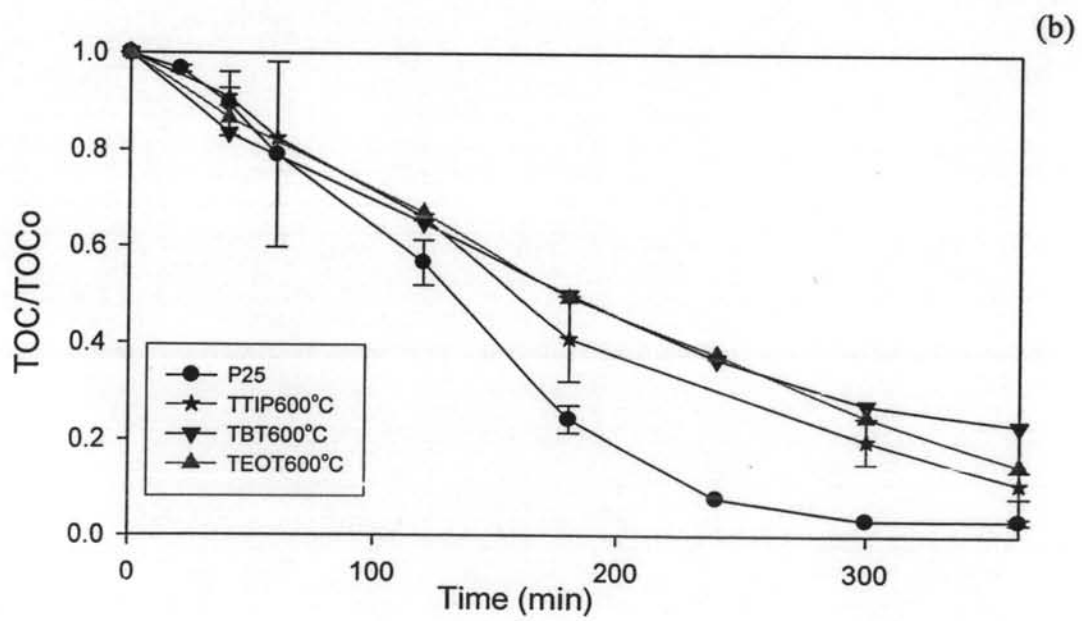
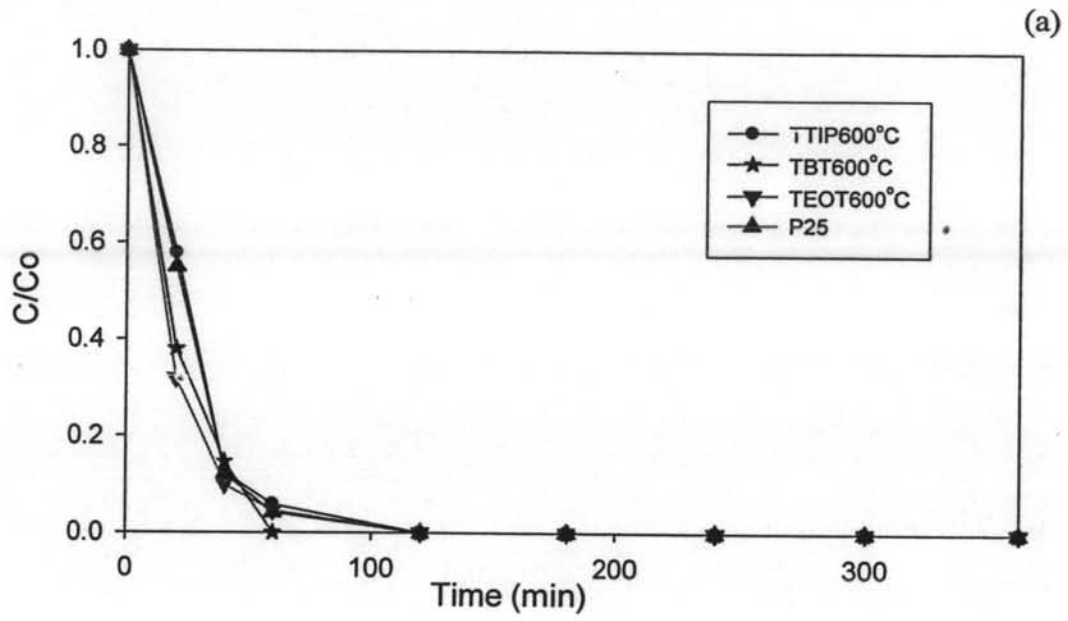
Figures 4.5-4.7 show the results for photocatalytic degradation of 4-CP by varying the type of Ti-precursor in the electrospinning process of  $\text{TiO}_2$  nanofibers at the calcination temperature 500, 600 and 700°C, respectively; and compared with Degussa P25. The decreasing of 4-CP remaining is very fast and disappears within 120 minutes for all types of catalysts even if without any catalysts (UV light alone). It indicates that  $\text{TiO}_2$  does not affect the 4-CP degradation. On the other hand, the UV light has a significant effect on the 4-CP degradation because with only visible light, the 4-CP remaining does not decrease at a significant level (Figure 4.5 (a)). However, from the TOC remaining, Degussa P25 has the highest photocatalytic activity as seen in Figures 4.5 (b), 4.6 (b) and 4.7 (b); the reduction of the TOC almost disappears after 360 minutes. It was found that after 360 minutes of the reaction, the TOC remaining of all types of Ti-alkoxide are about 0.2 or lower, so these results show the types of Ti-alkoxide have an insignificant effect on the reduction rate of the TOC reductions.

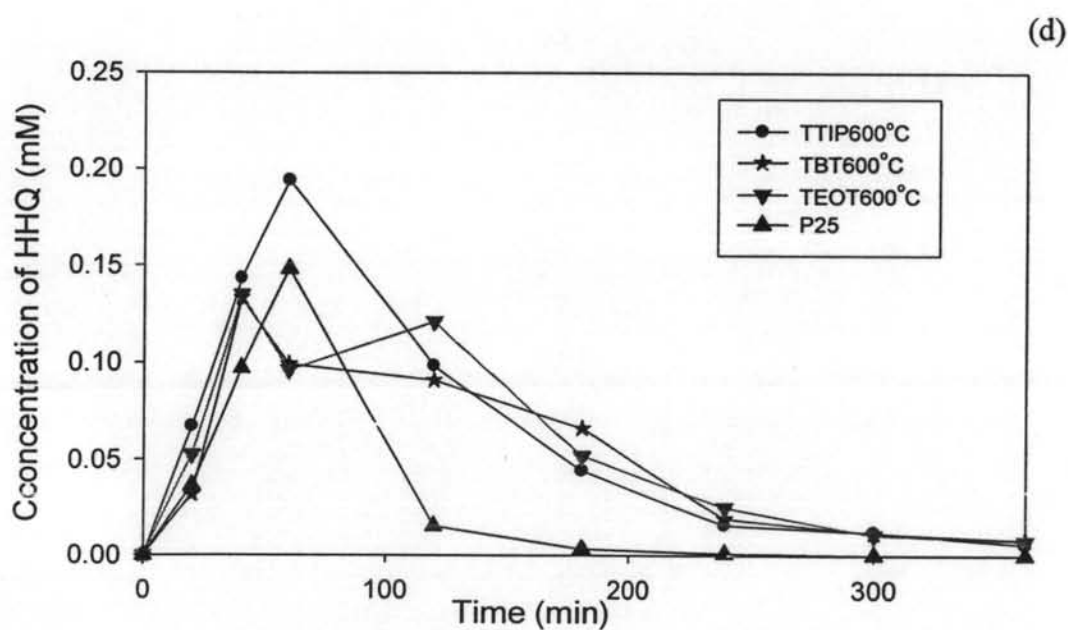
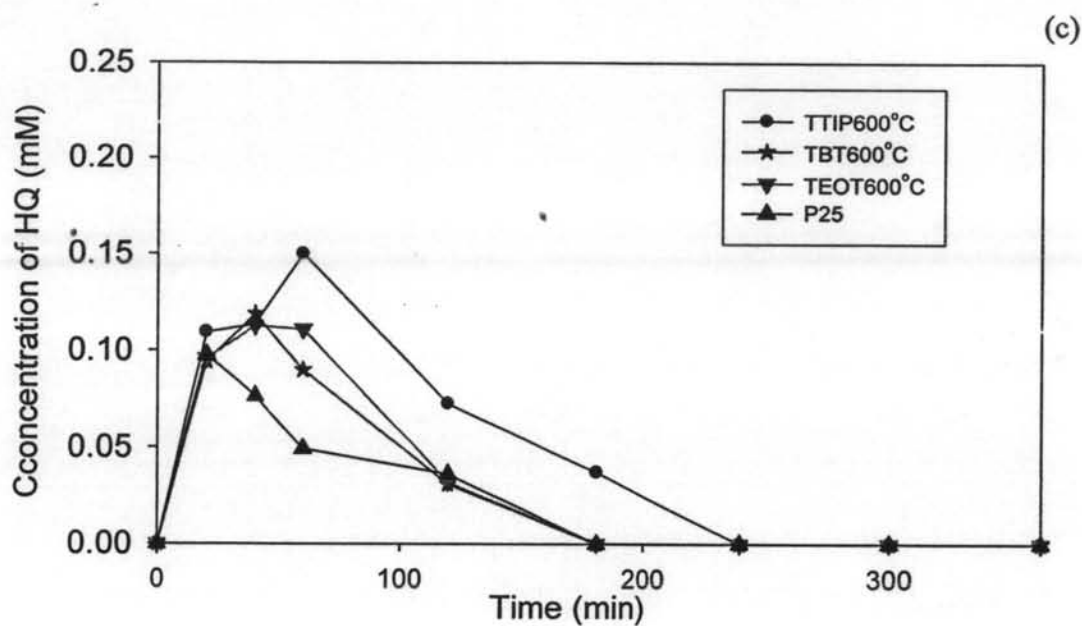
Intermediate products, HQ and HHQ, formed during the photocatalytic reaction are shown in Figures 4.5 (c-d), 4.6 (c-d) and 4.7 (c-d). Significant quantities of both HQ and HHQ can be observed within 120 minutes after the start of the reaction. In the case of Degussa P25, HQ and HHQ completely disappear after the irradiation for 180 and 240 minutes, respectively. For the  $\text{TiO}_2$  nanofibers from TTIP, TBT, and TEOT, HQ completely disappears after the irradiation for 300, 180, and 180 minutes, respectively. But HHQ still exists after 360 minutes. Moreover, the decomposition of HHQ is in agreement with the reduction of the TOC remaining for all types of catalyst.



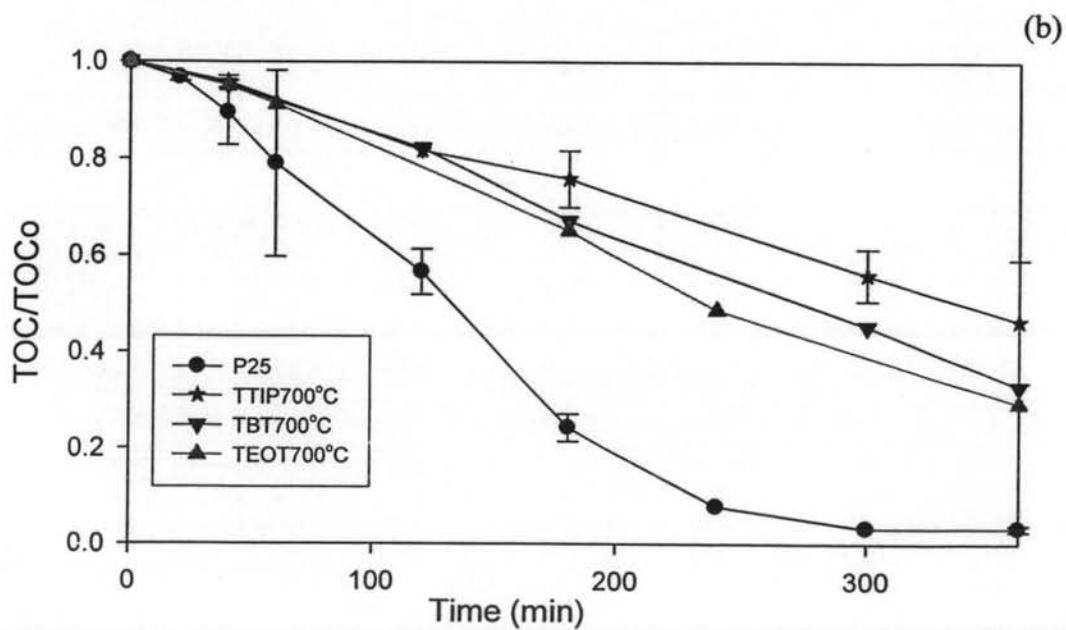
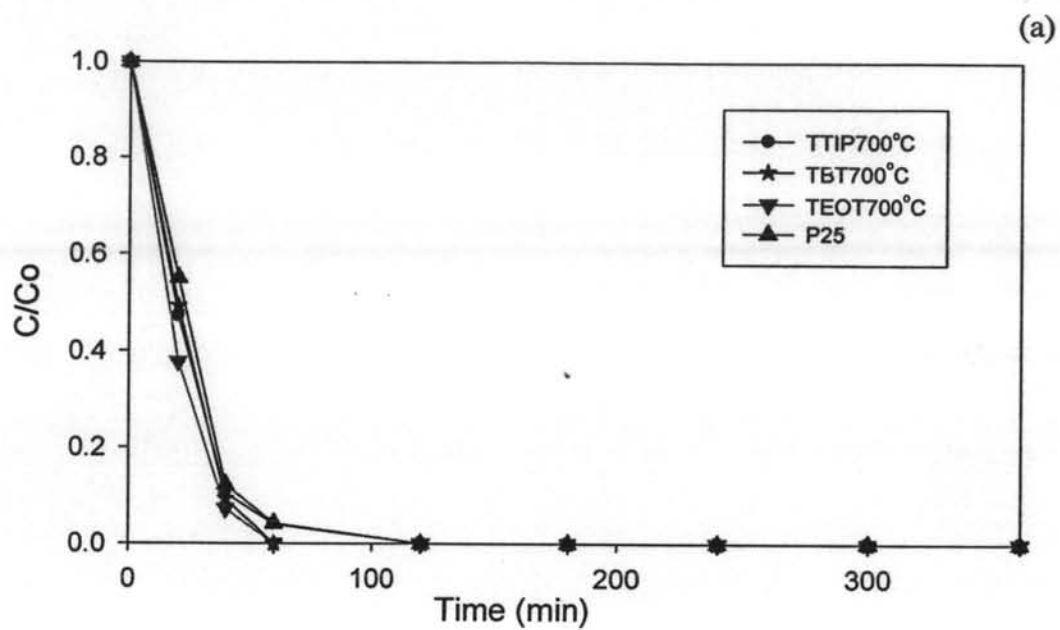


**Figure 4.5** Photocatalytic degradation of 4-CP as a function of irradiation time using the TiO<sub>2</sub> nanofibers prepared with different Ti-precursors after the calcination at 500°C and TiO<sub>2</sub> (Degussa P25) (a) remaining fraction of 4-CP (b) remaining fraction of TOC (c) concentration of HQ (d) concentration of HHQ.





**Figure 4.6** Photocatalytic degradation of 4-CP as a function of irradiation time using the TiO<sub>2</sub> nanofibers prepared with different Ti-precursors after the calcination at 600°C and TiO<sub>2</sub> (Degussa P25) (a) remaining fraction of 4-CP (b) remaining fraction of TOC (c) concentration of HQ (d) concentration of HHQ.



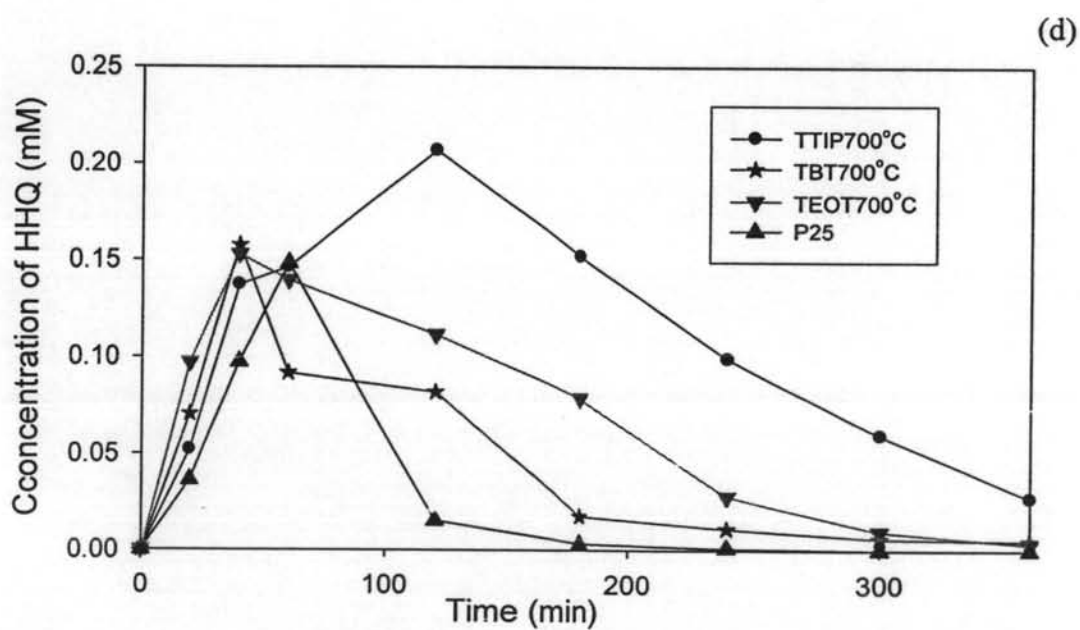
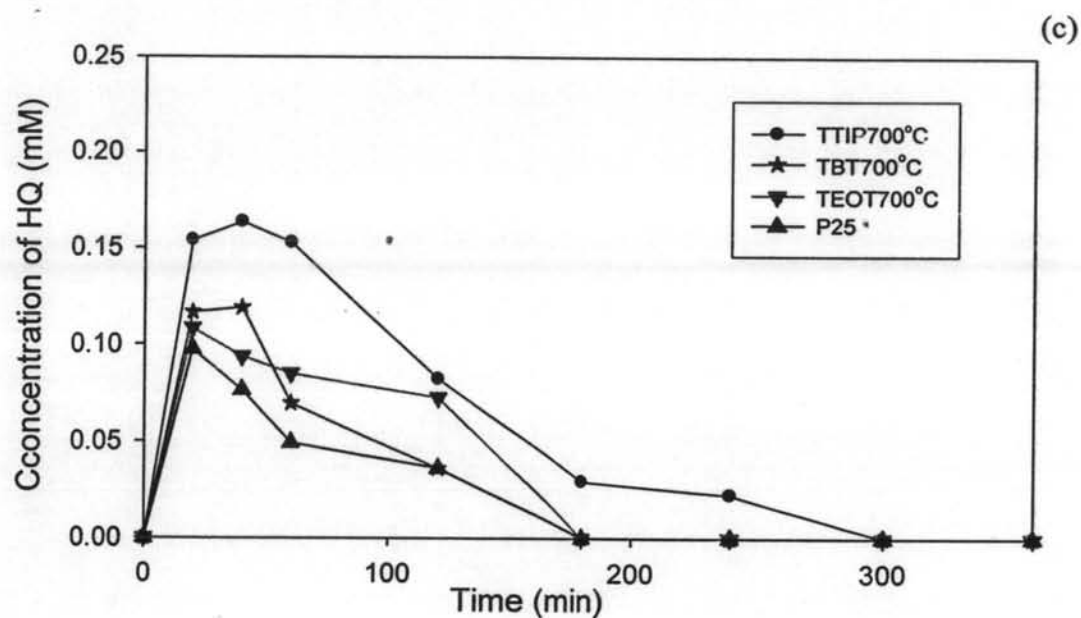


**Figure 4.7** Photocatalytic degradation of 4-CP as a function of irradiation time using the TiO<sub>2</sub> nanofibers prepared with different Ti-precursors after the calcination at 700°C and TiO<sub>2</sub> (Degussa P25) (a) remaining fraction of 4-CP (b) remaining fraction of TOC (c) concentration of HQ (d) concentration of HHQ.



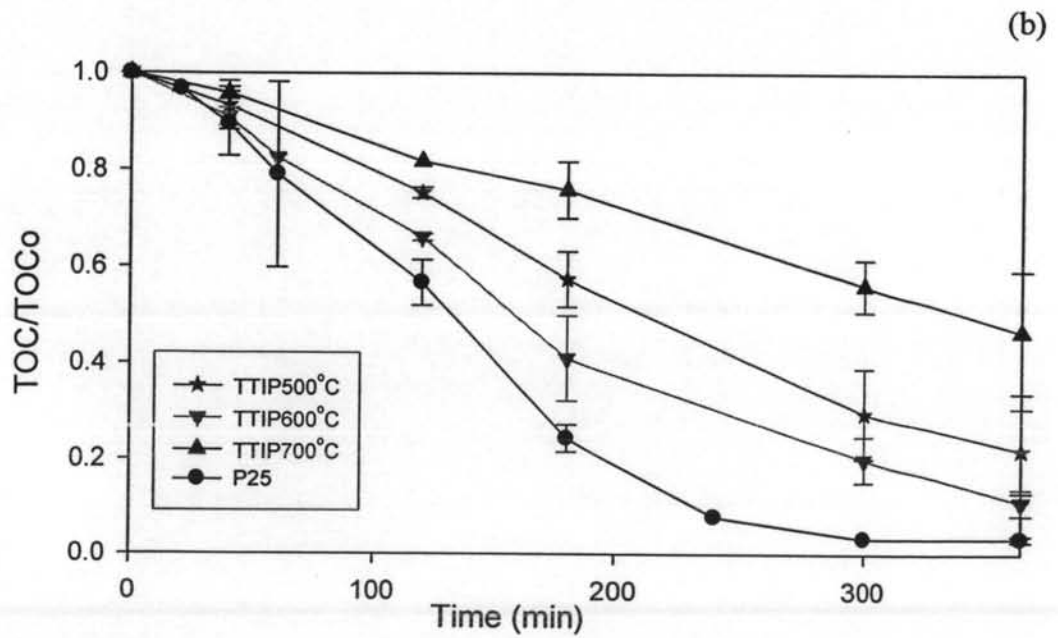
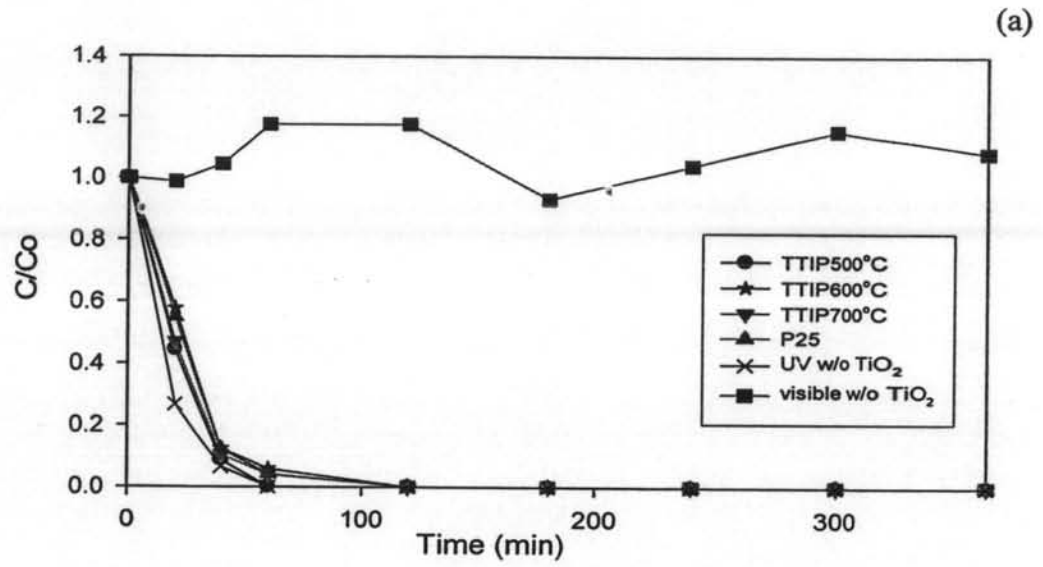
#### 4.2.2 Effect of Calcination Temperature

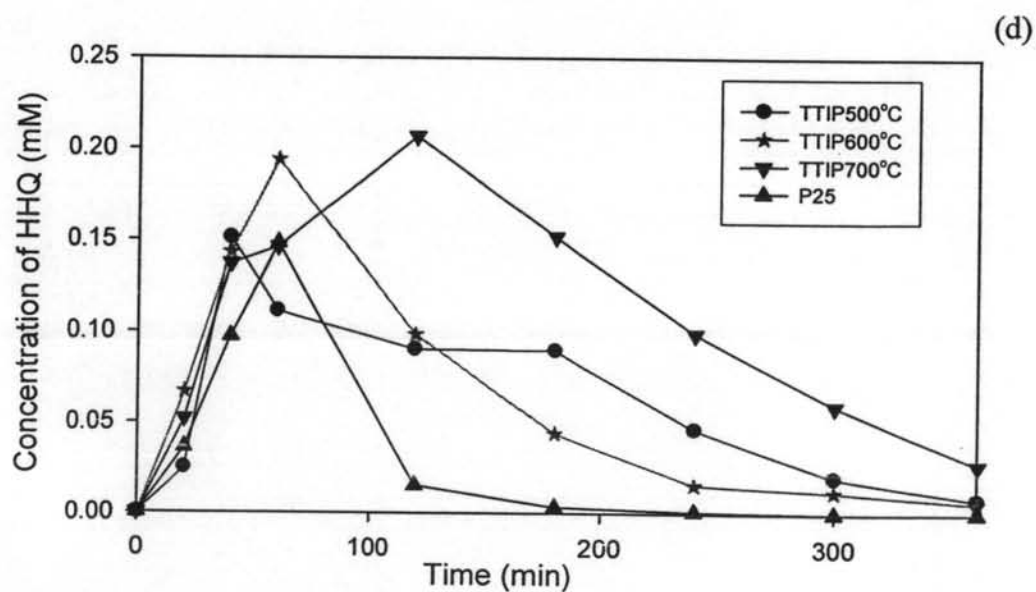
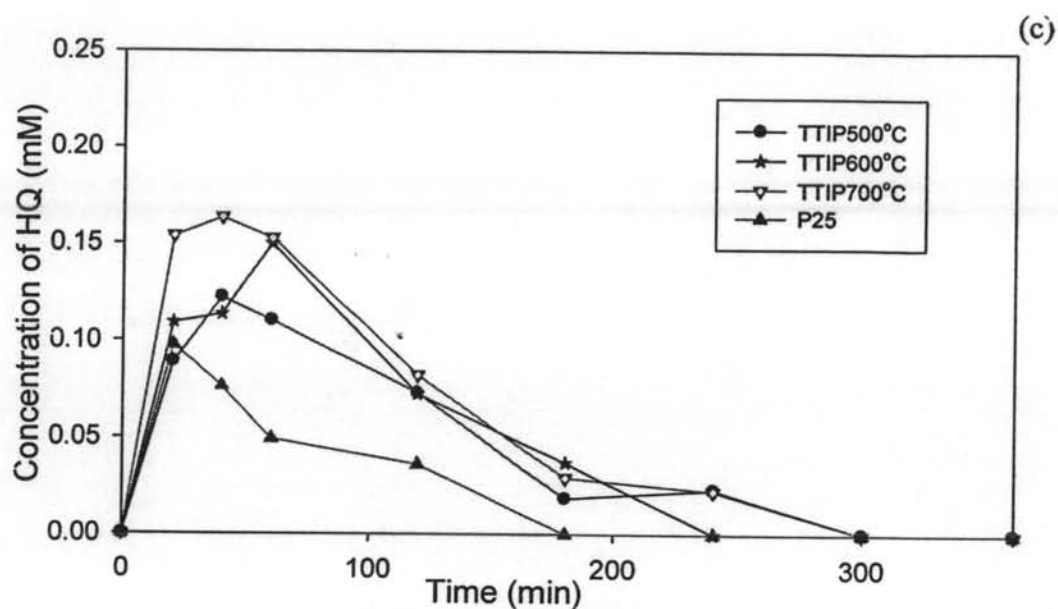
Figure 4.8 shows photocatalytic degradation of 4-CP from the TiO<sub>2</sub> nanofibers prepared from TTIP after the calcination at 500, 600, and 700°C. The reduction of the 4-CP is relatively constant even with the increase in the calcination temperature. But for the TOC remaining, with the increase in the calcination temperature from 500 to 600°C, the TOC/TOC<sub>0</sub> at 360 minutes decreases but it is still in the range of 0.2. As the calcination temperature increases to 700°C, the TOC remaining increases and the TOC/TOC<sub>0</sub> is higher than that of the calcination temperature at 500 and 600°C, because at 700°C, the rutile phase increases to the value of about 42% by the calcination temperature from 500 to 700°C.

Figures 4.9 (b) and 4.10 (b) show the TOC remaining in the case of TBT and TEOT at the calcination temperature of 500, 600, and 700°C, respectively. For both Ti-alkoxides, photocatalytic activities decrease with the increase in the calcination temperature. It can be explained by the decrease in the active surface area (BET) with the increase in the calcination temperature for both precursors.

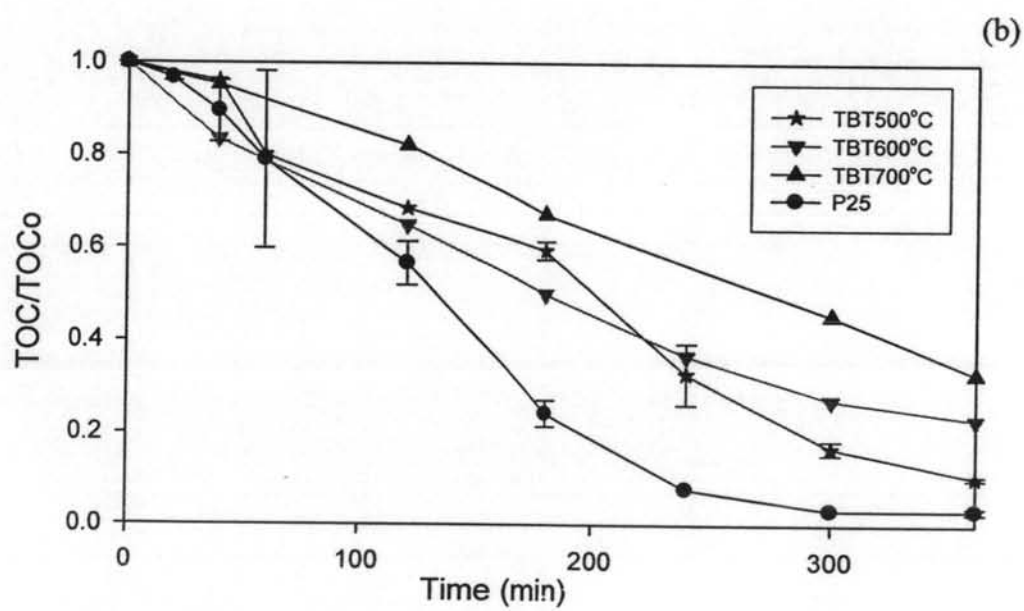
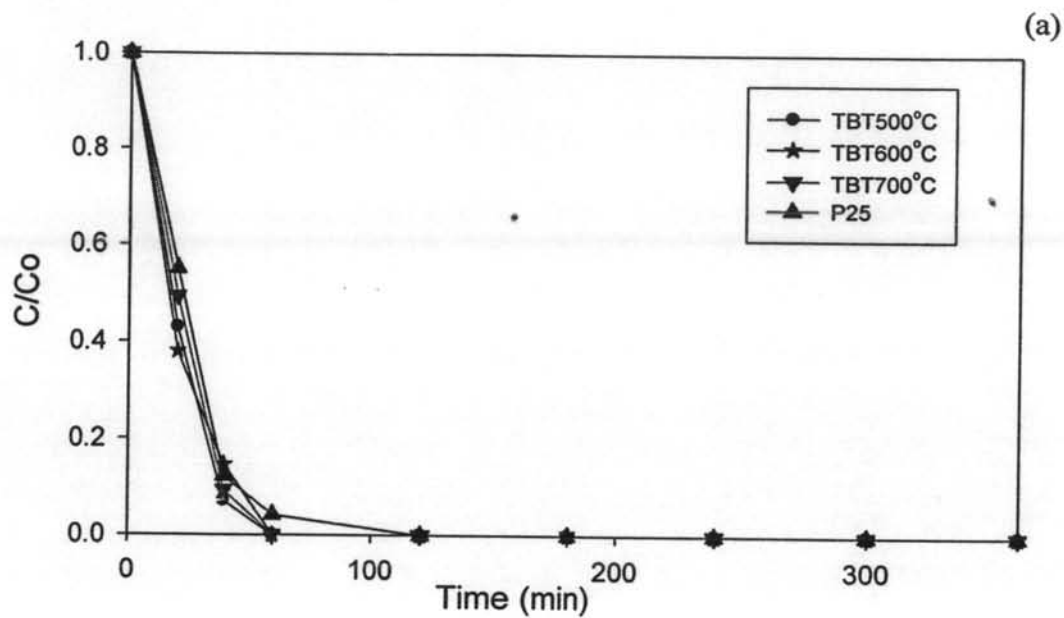
Figures 4.8 (c-d), 4.9 (c-d) and 4.10 (c-d) show the concentration profiles of HQ and HHQ during the photocatalytic reaction with difference calcination temperature for each Ti-alkoxide. It was found that with an increase in the calcination temperature of the catalysts, both HQ and HHQ are more difficult to be degraded, especially for the calcination temperature of 700°C. These results support the fact that the rutile phase is less active than the anatase phase. In addition, according to the crystallite size of anatase from the same types of precursor, it was found that in the case of using TBT and TEOT, an increase in the calcination temperature, both the anatase size and the TOC/TOC<sub>0</sub> increase. HQ decomposes more easily but HHQ decomposes more difficultly as the calcination temperature increases. It can be explained that the crystallite size of anatase has a significant effect on the degradation of the intermediate products. In the case of using TTIP, as increase in the calcination temperature from 500 to 600°C, the crystallite size of anatase decreases, but for the calcination temperature at 700°C, the crystallite size of anatase increases. Consequently, the lowest TOC remaining is obtained using TiO<sub>2</sub> from TTIP at the calcination temperature of 600°C.

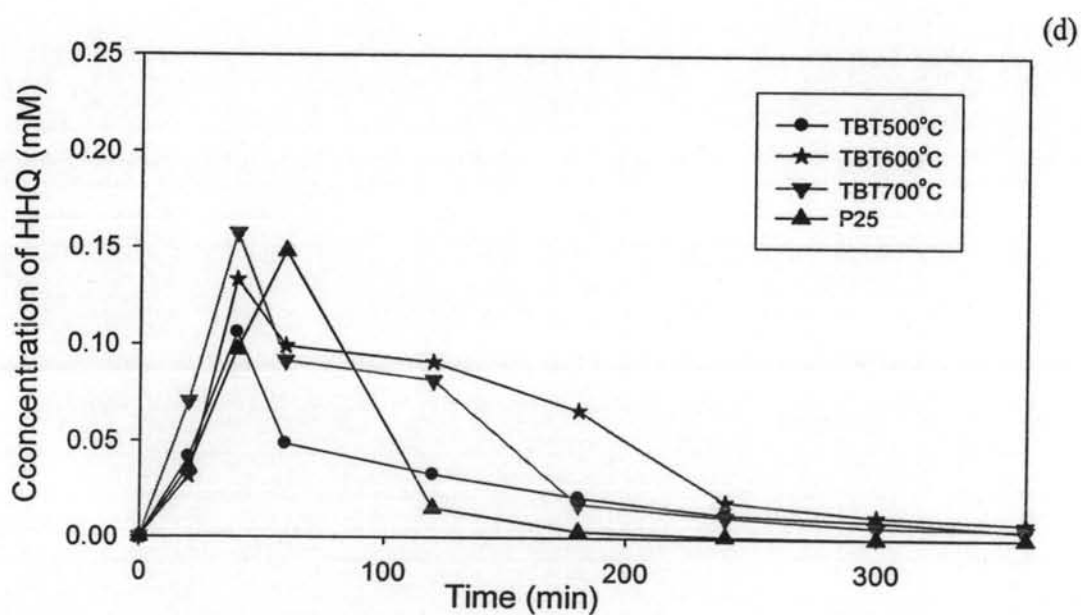
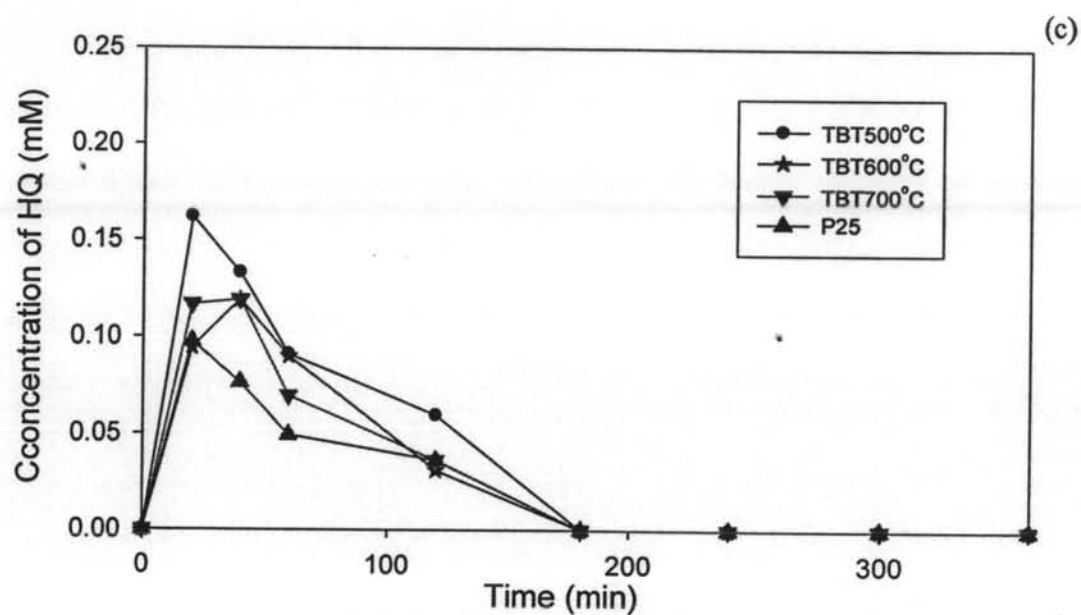
Although Degussa P25 has little percentage of rutile (about 20%), its efficiency in the degradation of HQ and HHQ is highest. This can be explained that there is a synergistic effect between contacting anatase and rutile phase (Sun and Smirniotis, 2003). A closer contact of the anatase and rutile particles induces the transfer of holes and electrons between the two phase; therefore, the  $e^-/h^+$  recombination is reduced (Wu *et al.*, 2004). As a right amount of each phase (the optimum rutile/anatase ratio) is expected for synergistic effect because further increase in the amount of the rutile phase results in lower active surface areas for photocatalytic activity.



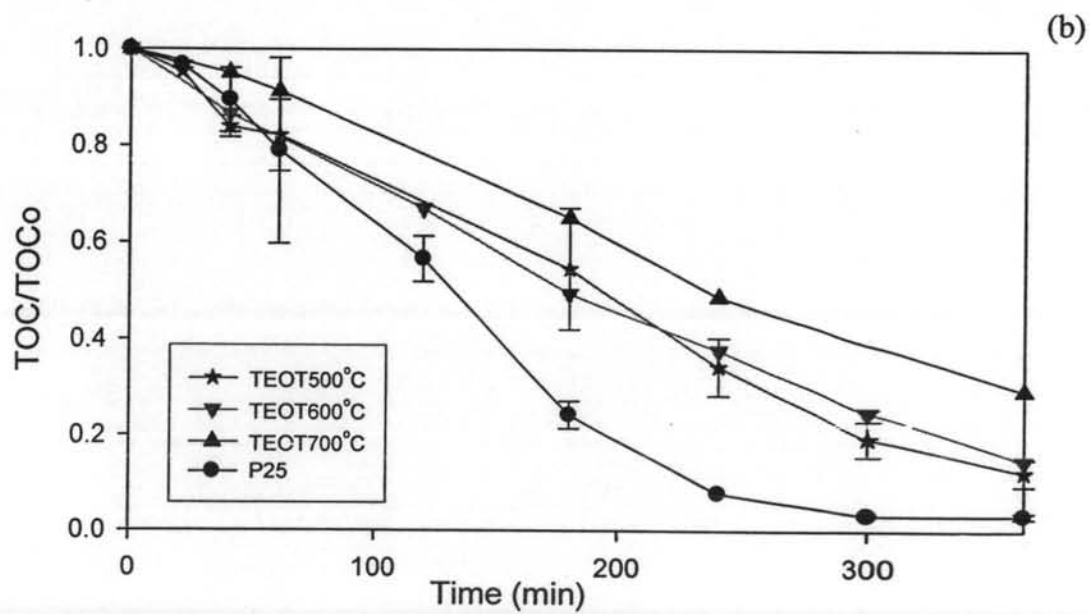
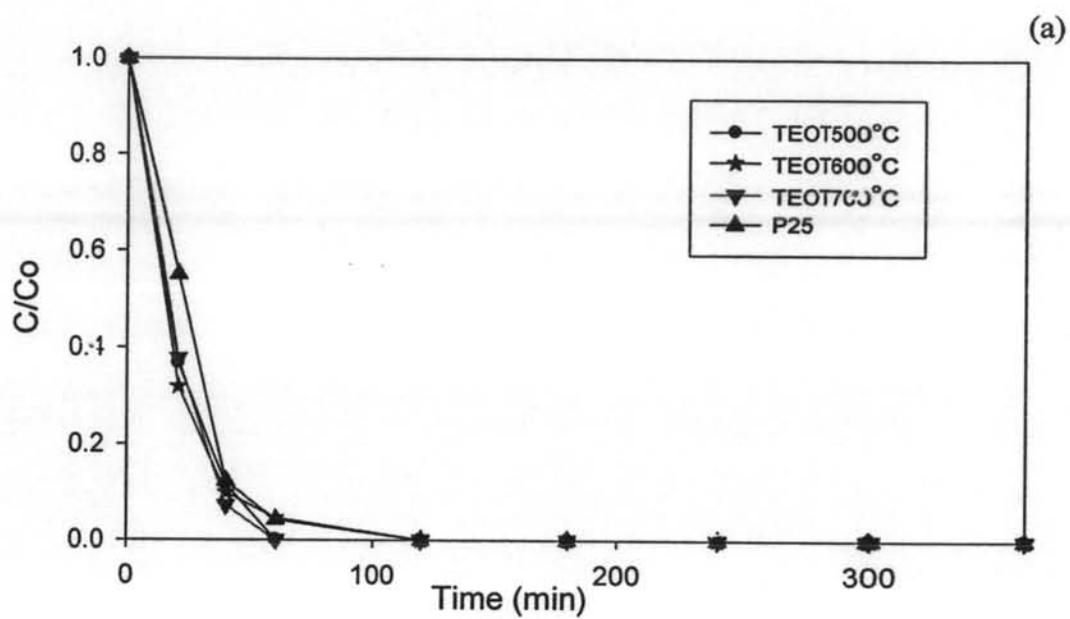


**Figure 4.8** Photocatalytic degradation of 4-CP as a function of irradiation time using the TiO<sub>2</sub> nanofibers prepared with the TTIP-precursor after the calcination at 500, 600, and 700°C and TiO<sub>2</sub> (Degussa P25) (a) remaining fraction of 4-CP (b) remaining fraction of TOC (c) concentration of HQ (d) concentration of HHQ.





**Figure 4.9** Photocatalytic degradation of 4-CP as a function of irradiation time using the TiO<sub>2</sub> nanofibers prepared with the TBT-precursor after the calcination at 500, 600, and 700°C and TiO<sub>2</sub> (Degussa P25) (a) remaining fraction of 4-CP (b) remaining fraction of TOC (c) concentration of HQ (d) concentration of HHQ.



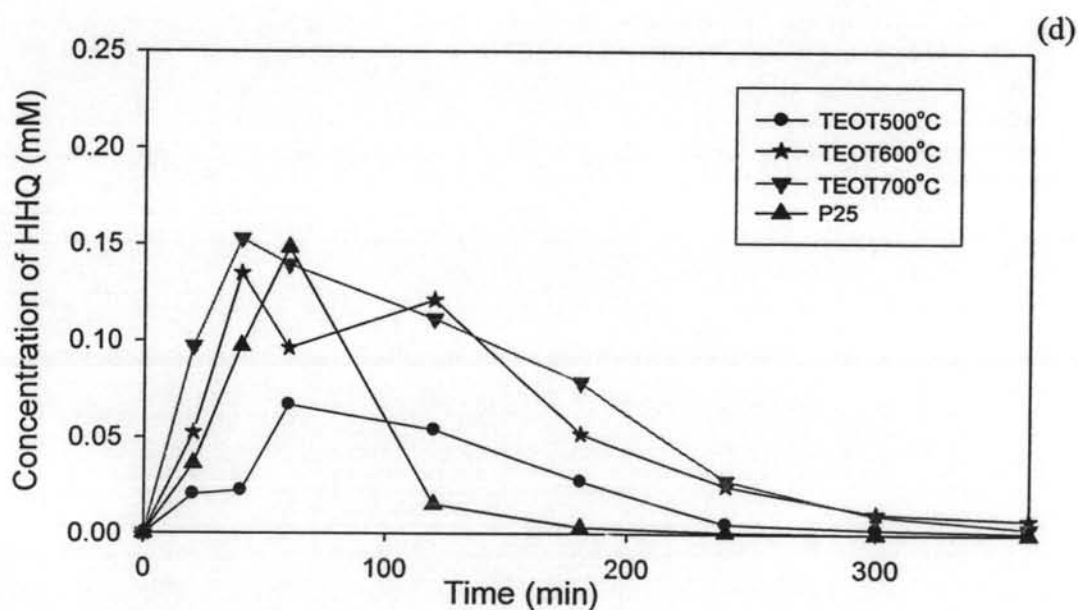
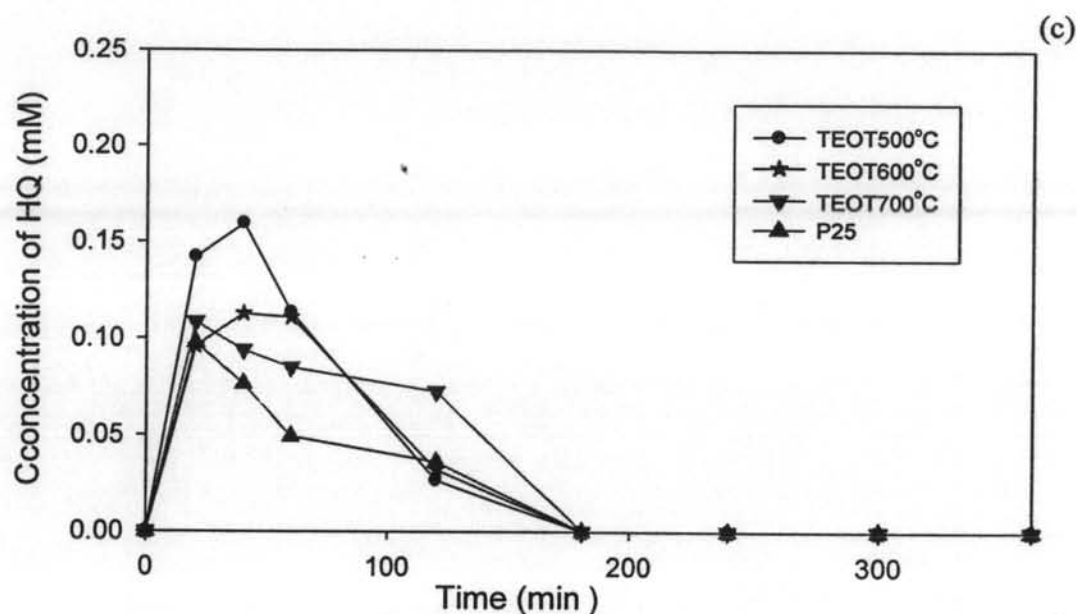


**Figure 4.10** Photocatalytic degradation of 4-CP as a function of irradiation time using the TiO<sub>2</sub> nanofibers prepared with the TEOT-precursor after the calcination at 500, 600, and 700°C and TiO<sub>2</sub> (Degussa P25) (a) remaining fraction of 4-CP (b) remaining fraction of TOC (c) concentration of HQ (d) concentration of HHQ.



#### 4.2.3 Effect of Metal Doping

In this section, TTIP was chosen as a precursor with 600°C calcination temperature because it has the lowest value of the TOC/TOC<sub>0</sub> at 360 minutes of the reaction.

Figure 4.11 shows the results for photocatalytic degradation of 4-CP by increasing the amount of Ag doped TiO<sub>2</sub> from 0 to 4 wt% of TiO<sub>2</sub> and compared with Degussa P25.

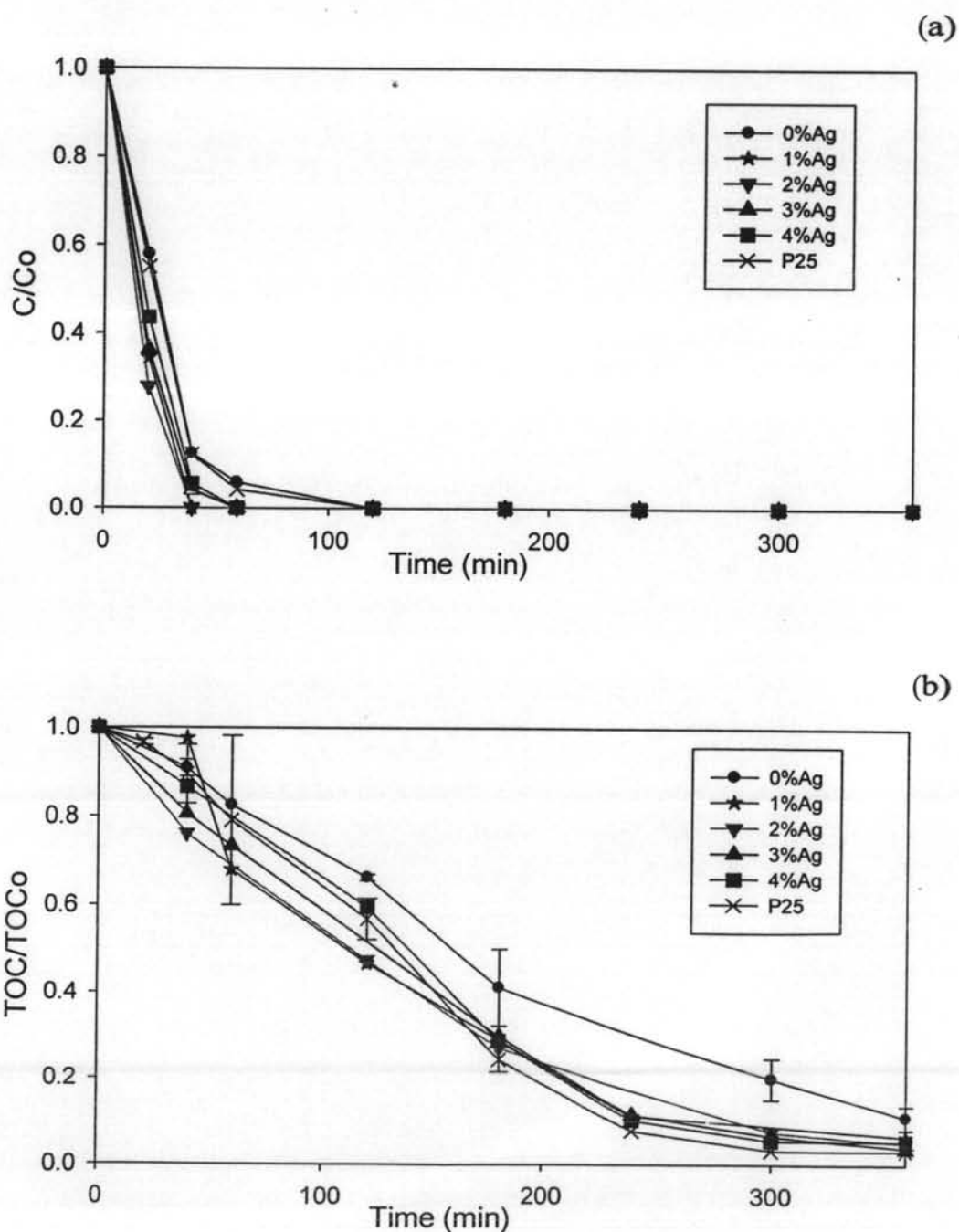
Figure 4.11 (a) shows the comparison of the reduction of 4-CP remaining with different amounts of Ag doping and Degussa P25. It was found that for 0%Ag/TiO<sub>2</sub> and Degussa P25, the 4-CP disappears within 120 minutes but for 1%-4%Ag/TiO<sub>2</sub>, C/Co disappears within 60 minutes. This suggests that doping some Ag can enhance the reduction of 4-CP. Figure 4.11 (b) shows that adding Ag increases the reduction of TOC to be close to that of using the Degussa P25. Furthermore, 0%Ag/TiO<sub>2</sub> has the lowest TOC reduction.

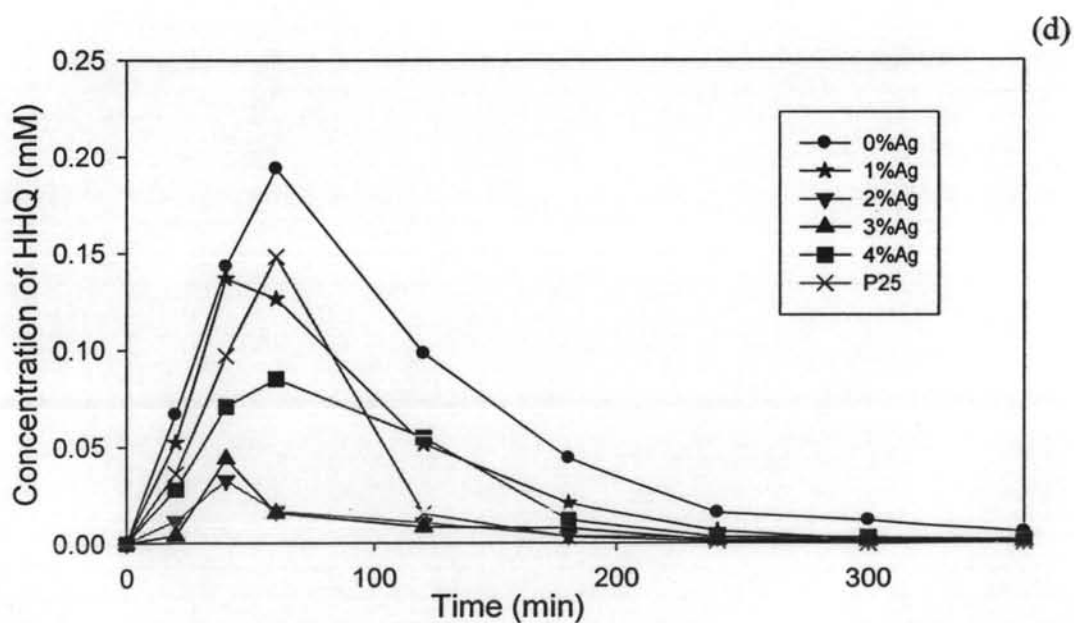
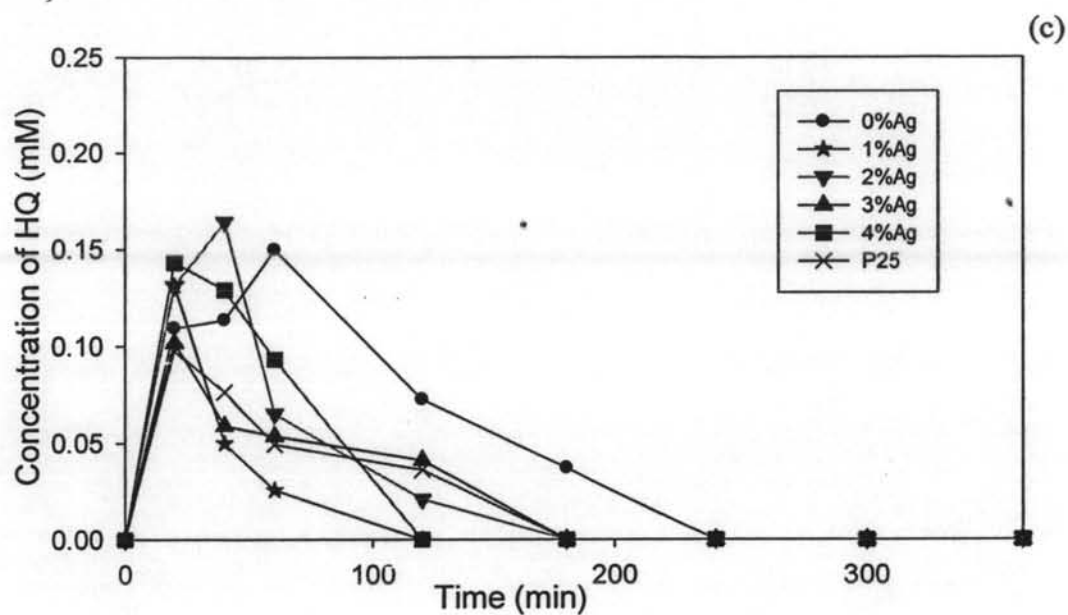
The concentrations of HQ and HHQ during the 360 minutes of reactions are shown in Figure 4.11 (c) and (d), respectively. It was found that for 0%Ag/TiO<sub>2</sub>, HQ disappears in 240 minutes, but using 1% to 4%Ag/TiO<sub>2</sub> and Degussa P25, HQ disappears more rapidly within 180 minutes.

The degradation of HHQ from Figure 4.11 (d) shows that with an increase in the amount of Ag from 0 to 3 wt% on TiO<sub>2</sub>, HHQ concentration decreases. But further increase in the amount of Ag to 4% on TiO<sub>2</sub>, the HHQ concentration increases. Although, for the Degussa P25, HHQ concentration between 0 and 120 minutes is higher than that with Ag doped TiO<sub>2</sub> at any percentages and completely disappears in 300 minutes. And that shows similar performance as that of the Degussa P25.

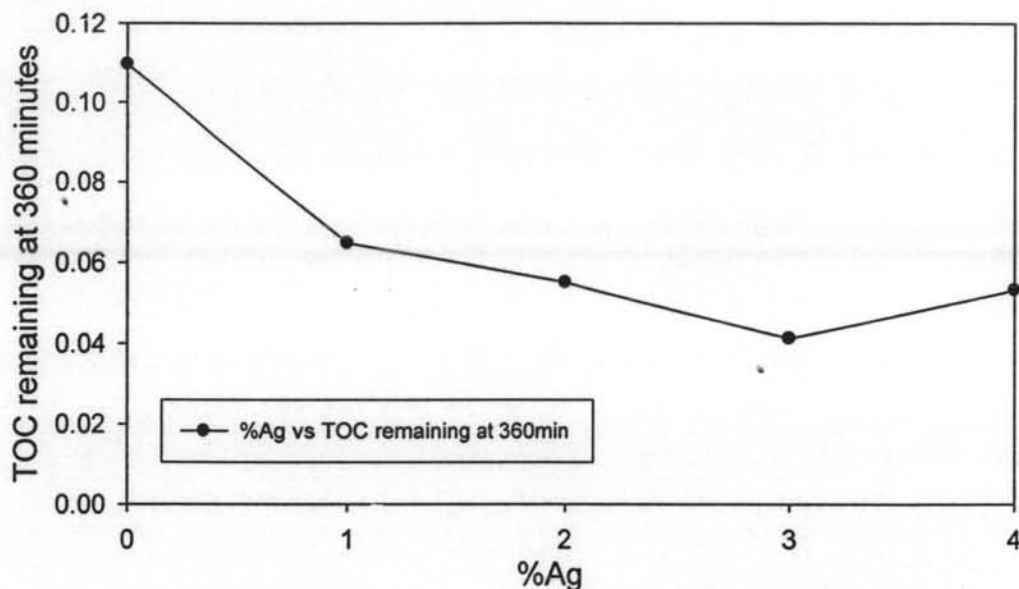
It is obvious that a small amount of Ag doping improves the photocatalytic activity (Thangsatjatham, 2004), because the small amount of Ag can accelerate the superoxide radical anion formation, O<sub>2</sub><sup>•-</sup>, which increases the lifetime of holes and suppresses the electron-hole recombination process (Blazkova *et al.*, 1998). The optimum percentage of Ag shown in Figure 4.12 is 1 wt%, because it shows that the TOC remaining fraction at 360 minutes of reactions is lower than 0%Ag/TiO<sub>2</sub>, and when adding more Ag, the TOC remaining fraction are quite the

same for every percentage of Ag. However, A slight increase of TOC/TOCo with 4%Ag/TiO<sub>2</sub> may be due to adding Ag too much can also block the active site that can be exposed to the UV light (Thangsatjatham, 2004). Another reason is when the amount of Ag increases to a certain level, the photo electron will transfer from the semiconductor to metal particles while the accumulated negative charge is not consumed or no further transferred out of the metal (Arabatzis *et al.*, 2003).



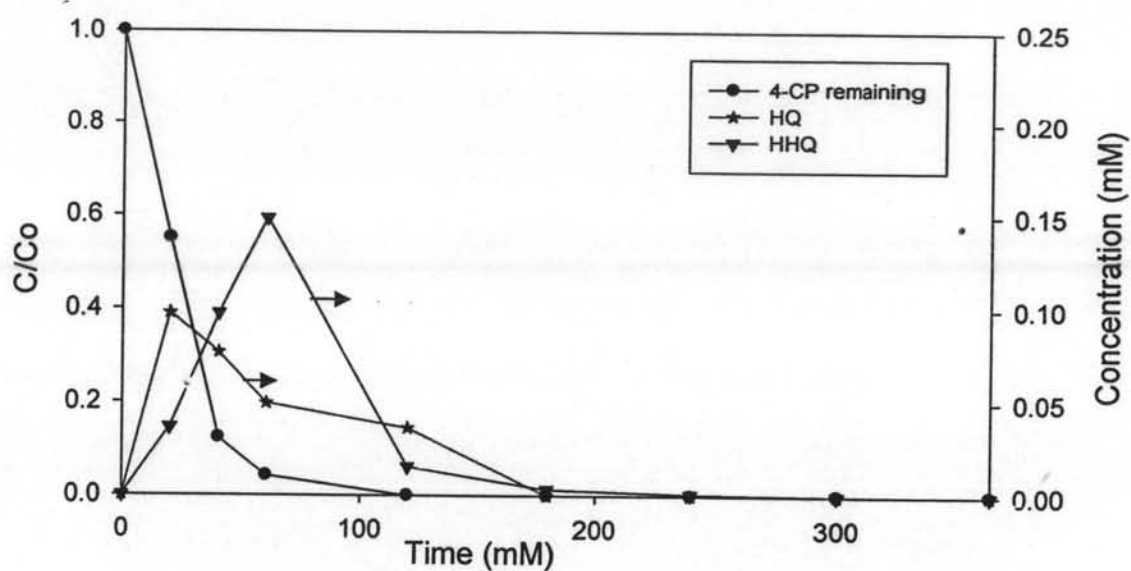


**Figure 4.11** Photocatalytic degradation of 4-CP as a function of irradiation time using the Ag doped  $\text{TiO}_2$  nanofibers and  $\text{TiO}_2$  (Degussa P25) (a) remaining fraction of 4-CP (b) remaining fraction of TOC (c) concentration of HQ (d) concentration of HHQ.

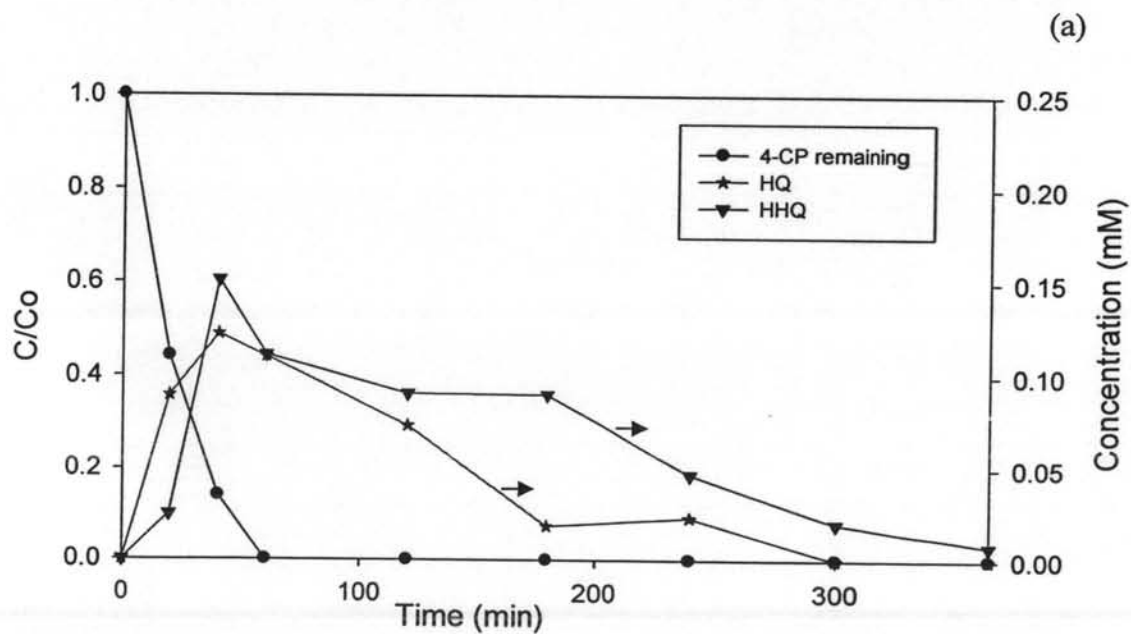


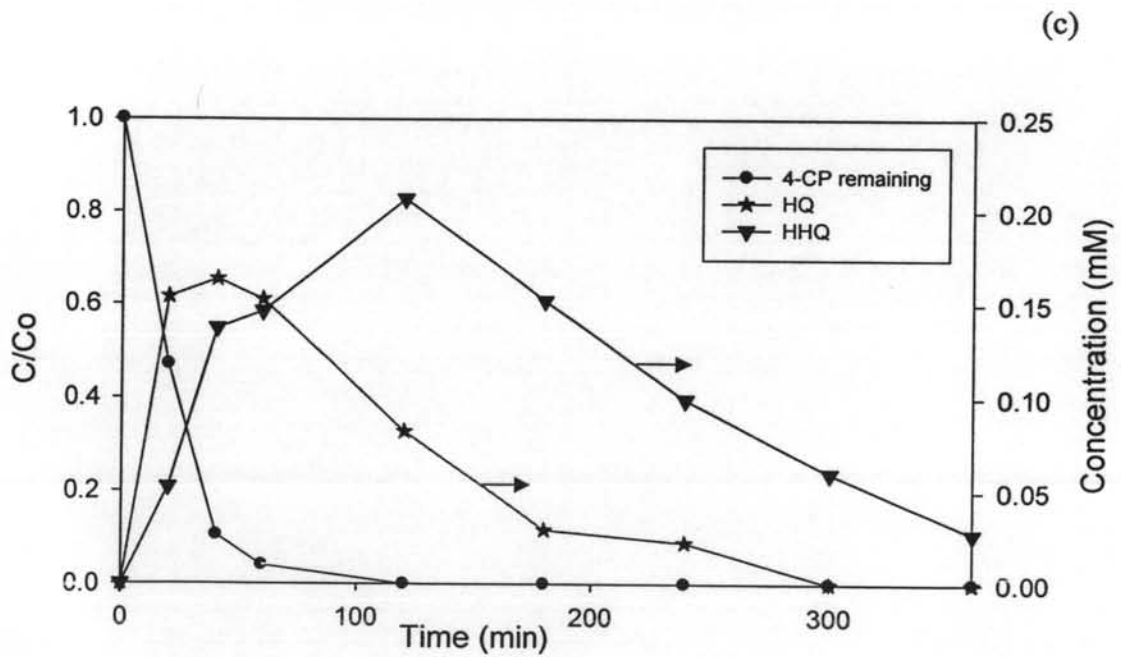
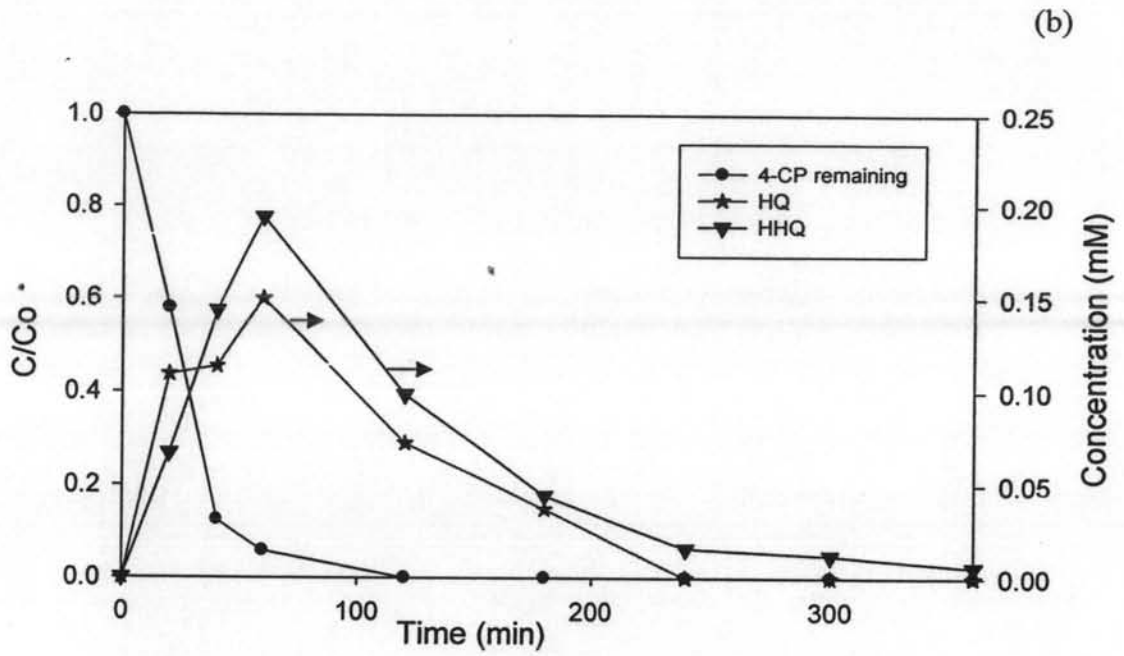
**Figure 4.12** Remaining fraction of TOC as a function of percent of Ag doped  $\text{TiO}_2$  at 360 minutes reaction time.

Figures 4.13 - 4.16 show the comparison of 4-CP remaining, HQ concentration and HHQ concentration using different types of catalysts. It was found that during the degradation of 4-CP, HQ starts to produce first followed by HHQ. The result can be explained by the HQ and HHQ concentration profiles. Both of them increase with increasing time and each system reaches the maximum point. After that, the concentration profiles tend to decrease. Interestingly, the slope of HQ is greater than that of HHQ. It indicates that HQ is produced as an intermediate product prior to the HHQ is produced. HQ Concentration starts to reduce first and disappears within 300 minutes, while the HHQ concentration reduces gradually and remains after 360 minutes of the reaction for all types of catalysts except the Degussa P25. From the results, it can be suggested that HHQ is a key intermediate for the photocatalytic degradation of 4-CP because it is more difficult to be decomposed to  $\text{CO}_2$  and  $\text{H}_2\text{O}$ .

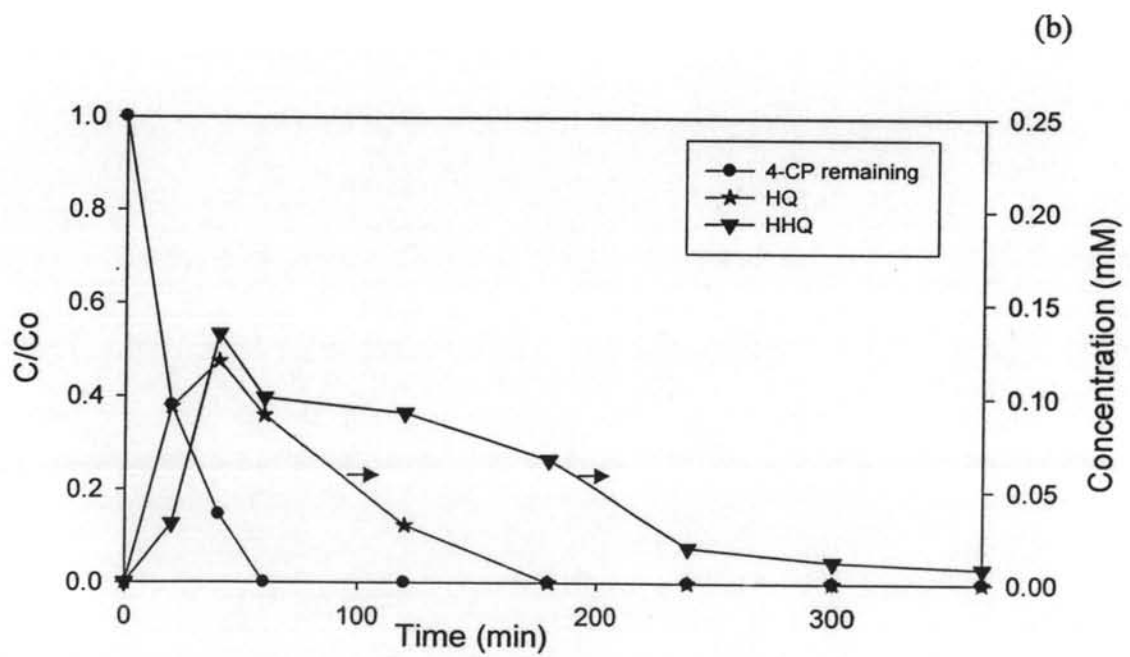
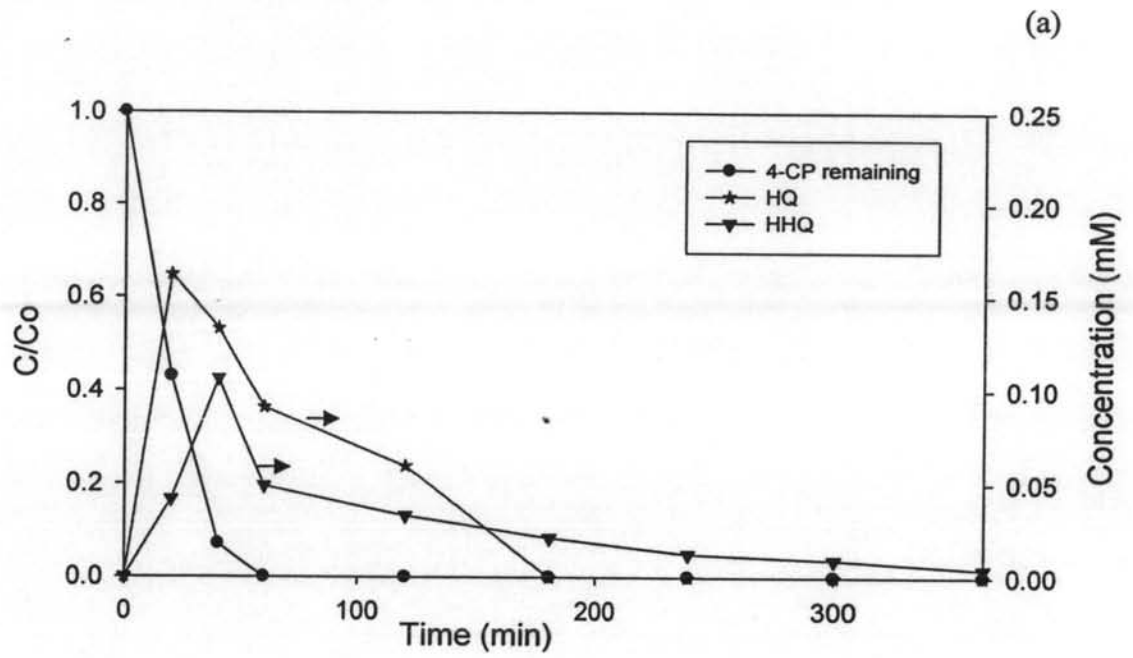


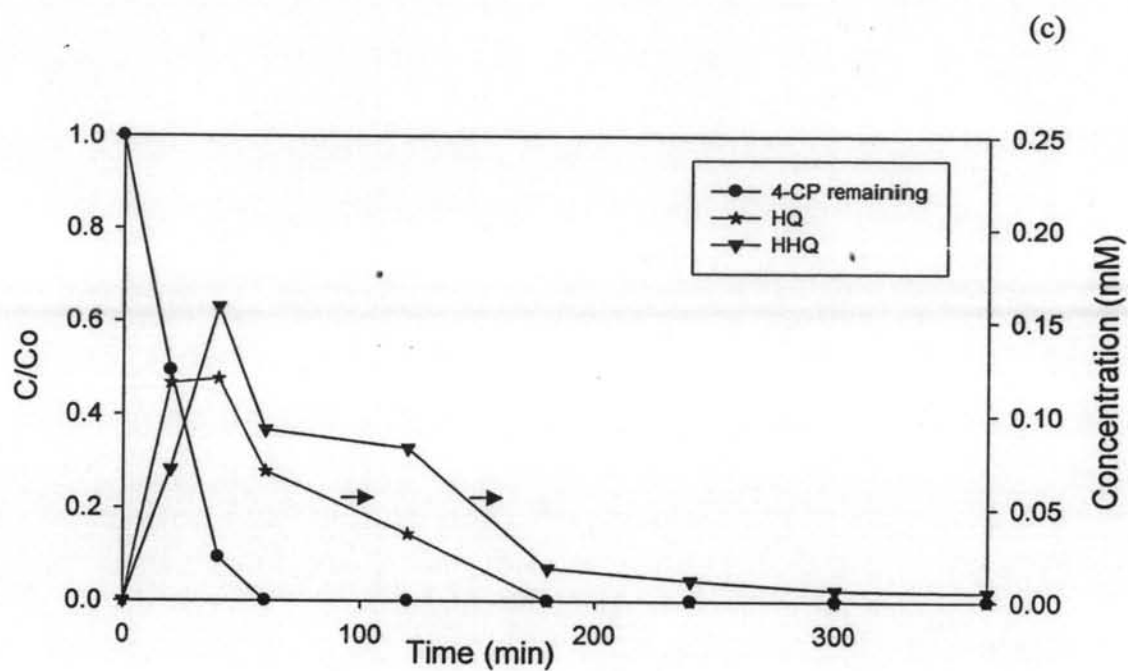
**Figure 4.13** Comparison of photocatalytic degradation of 4-CP and intermediates as a function of irradiation time using Degussa P25 as a photocatalyst.



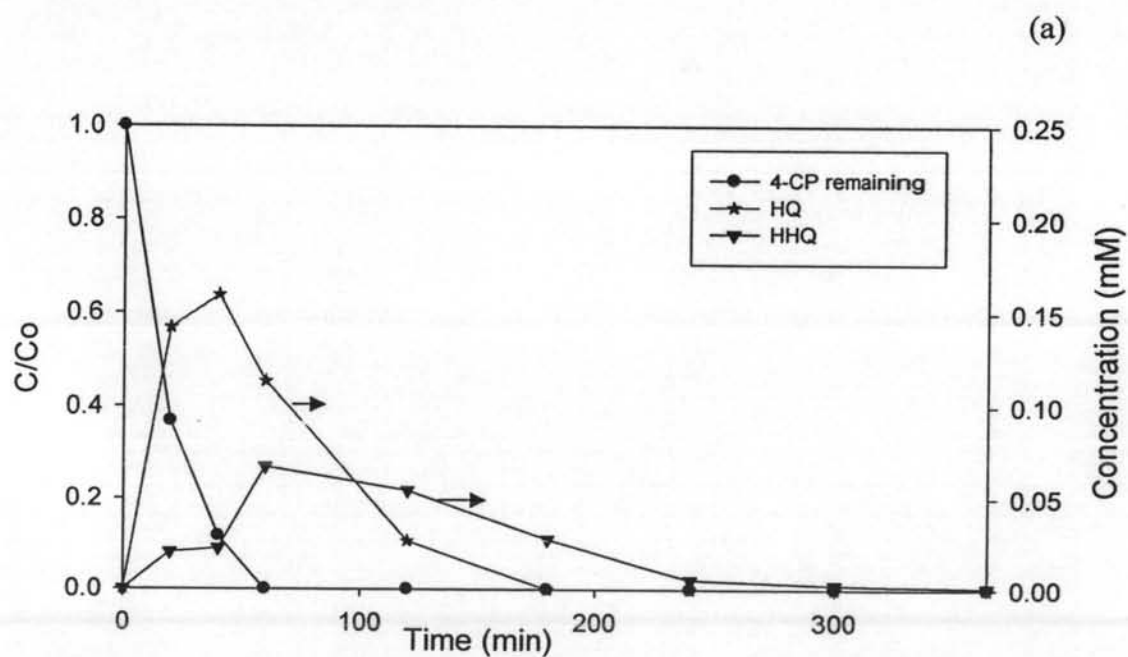


**Figure 4.14** Comparison of photocatalytic degradation of 4-CP and intermediates as a function of irradiation time using  $\text{TiO}_2$  nanofibers from TTIP with calcination temperature (a)  $500^\circ\text{C}$  (b)  $600^\circ\text{C}$  (c)  $700^\circ\text{C}$ .





**Figure 4.15** Comparison of photocatalytic degradation of 4-CP and intermediates as a function of irradiation time using  $\text{TiO}_2$  nanofibers from TBT with calcination temperature (a)  $500^\circ\text{C}$  (b)  $600^\circ\text{C}$  (c)  $700^\circ\text{C}$ .





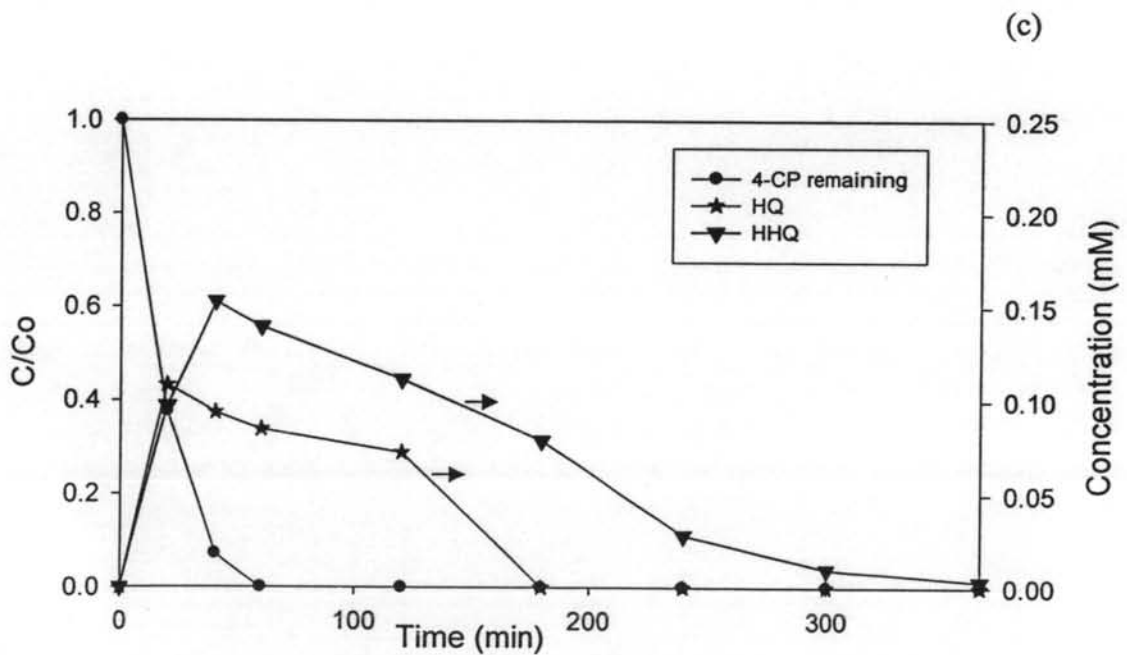
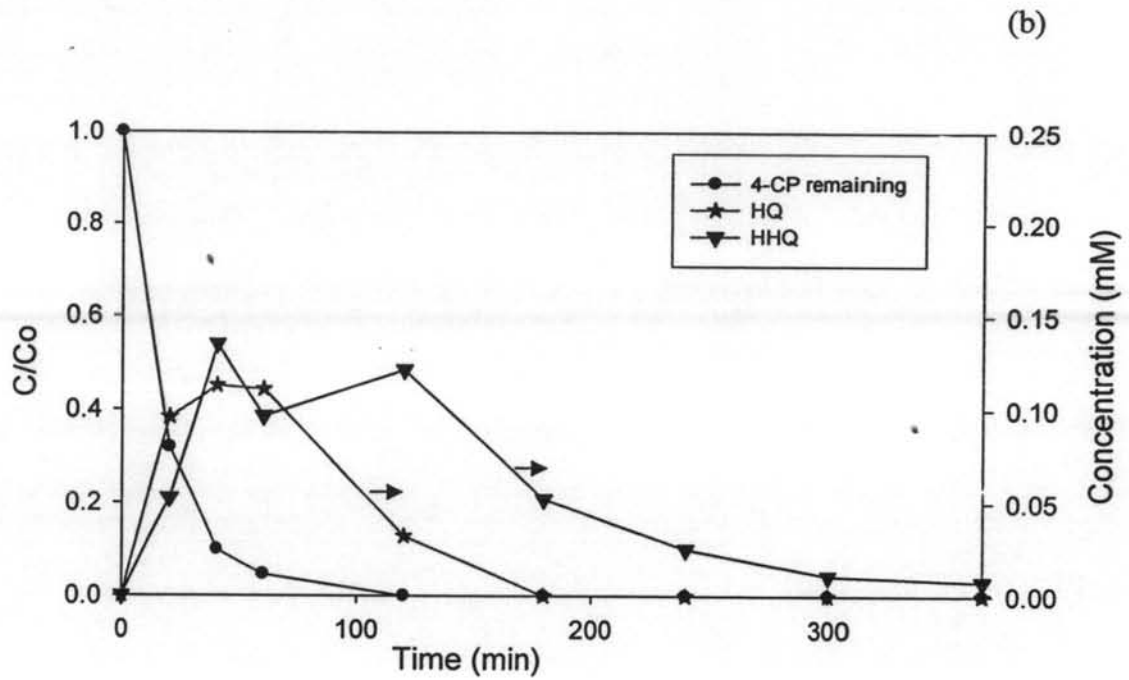


**Figure 4.16** Comparison of photocatalytic degradation of 4-CP and intermediates as a function of irradiation time using  $\text{TiO}_2$  nanofibers from TEOT with calcination temperature (a)  $500^\circ\text{C}$  (b)  $600^\circ\text{C}$  (c)  $700^\circ\text{C}$ .